AT&T Bell Laboratories Technical Journal
Vol. 63, No. 9, November 1984
Printed in U.S.A.

1982/83 End Office Connection Study: Analog Voice and Voiceband Data Transmission Performance Characterization of the Public Switched Network

By M. B. CAREY,* H.-T. CHEN,* A. DESCLOUX,* J. F. INGLE,* and K. I. PARK*

(Manuscript received December 19, 1983)

A comprehensive systemwide field study, referred to as the 1982/83 End Office Connection Study (EOCS), was undertaken by Bell Laboratories from October 1982 through January 1983 to characterize the transmission performance of the predivestiture Bell System public switched telecommunications network. Analog voice and voiceband data transmission parameters were measured on about 6500 direct-distance-dialing connections among 20 end office buildings located throughout the continental United States. The analog parameters measured on the connections included loss; noise; frequency response; envelope delay distortion; intermodulation distortion; phase jitter; amplitude jitter; peak-to-average ratio; frequency shift; propagation delay; transient phenomena such as impulse noise, gain hits, phase hits, and dropouts; and error rates of 1200-b/s full-duplex and 4800-b/s half-duplex data sets. This paper presents the results of the EOCS data analysis; a companion paper describes the measurement equipment and the sampling plan. The performance characterization information presented in this paper updates the similar information provided by a survey conducted in 1969/70. The results represent the last predivestiture Bell System network performance characterization and may serve as a benchmark for the end-to-end performance in the post-divestiture environment.

* AT&T Bell Laboratories; present affiliation Bell Communications Research, Inc.

Copyright © 1984 AT&T. Photo reproduction for noncommercial use is permitted without payment of royalty provided that each reproduction is done without alteration and that the Journal reference and copyright notice are included on the first page. The title and abstract, but no other portions, of this paper may be copied or distributed royalty free by computer-based and other information-service systems without further permission. Permission to reproduce or republish any other portion of this paper must be obtained from the Editor.

I. INTRODUCTION

Bell Laboratories undertook a comprehensive systemwide field study from October 1982 through January 1983 to characterize the transmission performance of the predivestiture Bell System public switched telecommunications network. This study, hereinafter referred to as the 1982/83 End Office Connection Study (EOCS), employed special measurement equipment, referred to as ASPEN (Automatic System for Performance Evaluation of the Network). Analog voice and voiceband data transmission parameters were measured on 6141 Direct-Distance-Dailing (DDD) connections among 20 end office buildings located throughout the continental United States; in addition, another 395 connections were measured among four pilot study locations at the start of the study. (Several end office buildings visited in the EOCS had multiple end office switches. When multiple switches were measured in the same building, they were individually identified in the EOCS database.) Measurements were typically made in one direction on each test connection. However, measurements were often made in both directions and sometimes repeated for stationarity studies, resulting in over 9000 1004-Hz loss measurements, for example.

The ASPEN equipment consisted of 20 Remote Test Units (RTUs) (one per sampled end office building) under the control of a computer located at Holmdel, New Jersey. Each RTU was connected to the line side of the main distributing frame in its central office and contained a microprocessor, a transmission impairment measuring set, and modems for communication with the central computer and for data performance tests. The transmission impairment measuring set (HLI 3701 Communications Test Set) was designed to meet the requirements specified in AT&T PUB 41009[1] for measuring the impairments described in AT&T PUB 41008.[2]

Analog parameters measured on the connections included loss, noise, frequency response, envelope delay distortion, intermodulation distortion, phase jitter, amplitude jitter, Peak-to-Average Ratio (P/AR), frequency shift, propagation delay, and transient phenomena such as impulse noise, gain and phase hits, and dropouts. Error rates of voiceband data sets were also measured for 1200-b/s full-duplex and 4800-b/s half-duplex transmission. Table I contains a complete list of the EOCS measurement parameters.

This paper presents the results of the EOCS data analysis; a companion paper[3] describes the ASPEN measurement equipment and the sampling plan. The performance characterization information presented in this paper updates similar information provided by the 1969/70 Connection Survey.[4] Furthermore, with the 1984 divestiture of the Bell System, the results represent the last predivestiture Bell System

Table I—Parameter coverage

Classification	Measured Parameter
Voice and voiceband data transmission	1004-Hz insertion loss Frequency response (30 frequencies) C-message noise Propagation delay Call cutoffs
Voiceband data transmission	Signal-to-C-notched-noise ratio C-notched noise 3-kHz flat noise 3-kHz flat notched noise 3-kHz noise-to-ground Envelope delay distortion (30 frequencies) P/AR Second-order intermodulation distortion Third-order intermodulation distortion Phase jitter (2 to 300 Hz) Phase jitter (20 to 300 Hz) Amplitude jitter (2 to 300 Hz) Amplitude jitter (20 to 300 Hz) Frequency shift Impulse noise (six thresholds) Phase hits (three thresholds) Gain hits (three thresholds) Dropouts
Data set error performance	1200-b/s bit error rate (two modems) 4800-b/s bit error rate (two modems) 1200-b/s block error rate (two modems) 4800-b/s block error rate (one modem)

network performance characterization and may serve as a benchmark for the end-to-end performance in the post-divestiture environment.

II. THE DATA ANALYSIS METHOD

The primary goal of data analysis in the EOCS was to provide estimates of the distributions of the parameters for various strata of interest and for the overall network. Estimation of the distribution was selected, since other measures such as means, variances, and quantiles are obtained as a function of the distribution.

The sampling design of the EOCS involved a stratification according to two variables:[3] connection airline mileage and type of switch at the end office. An analysis of covariance (with switch type as factor and mileage as covariate)[5] was carried out on each parameter to determine the effects of these two variables. Although the effects of mileage and switch type were often both significant at the 5-percent level, one effect usually dominated the other for the value of its F-statistic in the covariance model. Results are displayed as a function of the most relevant effect.

When a display as a function of airline mileage is deemed necessary, the results are split into three categories: short (0 to 180 miles),

medium (181 to 720 miles), and long (>720 miles). These particular mileage bands were chosen so that the EOCS results could be compared with similar results from the 1969/70 Connection Survey.[4]

The number of measurements varies with the measured parameter. To give an idea of the number of measurements taken for different strata, the number of 1004-Hz loss measurements made in the EOCS is shown in Fig. 1 as a function of airline mileage in 100-mile blocks, where the abscissa shows the midpoints of the 100-mile blocks (e.g., 5 represents the 451- to 550-mile block). Table II gives the number of 1004-Hz loss measurements in the EOCS for the short, medium, and long mileage categories, together with the number of different pairs of end office buildings evaluated in the EOCS. The estimated percentage of toll traffic[6] in each of the three mileage bands is also listed. Table III shows the number of 1004-Hz loss measurements made in the EOCS for each of the three types of switch—electronic switching system (digital switch), crossbar, and step-by-step switches—in the measuring end office, as well as the percentage of toll traffic estimated in each of the three switch strata.[7]

Table II—Stratification of data by connection airline mileage

Designation	Airline Mileage	Estimated Route Mileage	Number of Loss (1004-Hz) Measurements	Number of Nonordered Pairs of Sites	Percent of Toll Traffic
Short	0–180	0–341	776 8.1%	11 5%	77.8
Medium	181–720	342–1064	3717 38.8%	76 34.2%	13.4
Long	721–2576	1065–3378	5088 53.1%	135 60.8%	8.8
Total			9581	222	

Table III—Stratification of data by type of switch in the office where measurements were made

Designation	Number of Loss (1004-Hz) Measurements	Percent of Toll Traffic
Digital switch	4154 43.3%	58
Crossbar	4146 43.3%	30
Step-by-step	1281 13.4%	12
Total	9581	

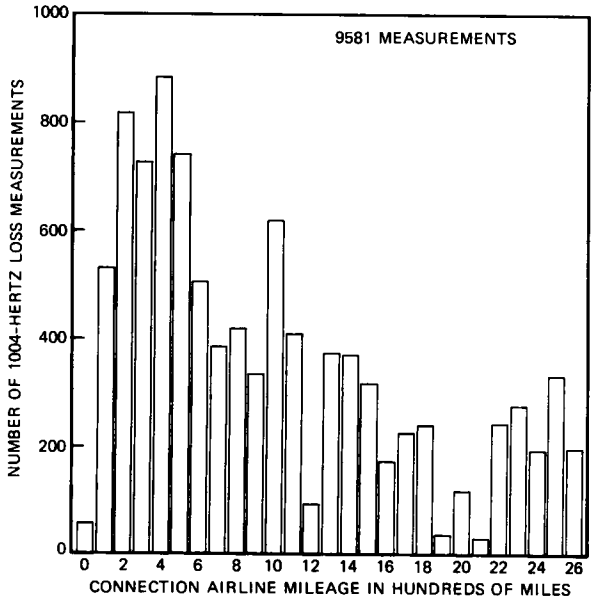

Fig. 1—Number of 1004-Hz loss measurements versus connection airline mileage in 100-mile blocks.

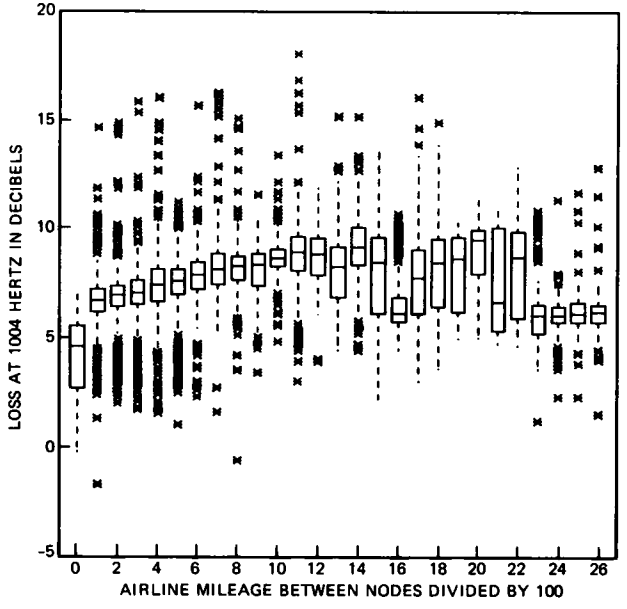

Fig. 2—The 1004-Hz loss versus connection airline mileage in 100-mile blocks.

Within each stratum, the measurements were considered self-weighted. Weights proportional to the traffic occurring in each stratum were used for calculation of results relevant to the whole network. A statistical model of components of variance was considered within each stratum for each parameter. The model led to the estimation of the variability of a parameter on a given pair of end office buildings, and of the variability between different pairs of end office buildings. These two variabilities, together with the means, are displayed in Table IV for all EOCS parameters other than the transient parameters. The variabilities are taken into consideration in the evaluation of the 90-percent confidence interval around the mean in each of the three mileage band strata, also shown in Table IV.

One goal of this paper is to characterize, where possible, the customer-premises-to-customer-premises performance, i.e., the end-office-to-end-office connection plus two loops. However, the impairment contributions from customer loops to the overall connection are usually negligible for most of the parameters discussed here. Therefore, the characterization information presented in this paper is, for the most part, based on the information available for end-office-to-end-office connections only, i.e., the EOCS results. However, for 1004-Hz loss, frequency response, and C-message noise, for which loops are significant, loop impairment contributions are concatenated to the end office to end office values, using a common source of information for the loop impairments, the 1980 Loop Survey.[8]

To concatenate the loop effects for loss and noise, distributions for 1224 predivestiture Bell System representative loops for 1004-Hz loss (measured at the main distributing frame) and C-message noise (measured at the customer premises) were extracted from the 1980 Loop Survey. Loop loss values were available at only three frequencies from that survey, so loop frequency responses were calculated from the transfer characteristics of loops obtained from the record survey associated with the 1980 Loop Survey. The distribution of a parameter for customer-premises-to-customer-premises connections was then obtained by analytically concatenating (using discrete convolution techniques) the distributions of the parameter on the loops with the distribution of the same parameter on the end-office-to-end-office connections. For frequency response, this concatenation process was repeated at each frequency.

III. RESULTS

All test signals were transmitted from the RTUs at −12 dBm.

3.1 1004-Hz loss

A 1004-Hz tone at −12 dBm was applied to one end of the connection, and the received level at the other end was measured, with the

difference in levels being defined as the loss of the connection. (If a tone of exactly 1000 Hz [an integer submultiple of the 8000-Hz sampling rate in time-division multiplex systems] were used, the loss readings would "bobble" by +/− 0.25 dB, the signal-to-C-notched-noise ratio readings would vary by +/− 5 dB, and the jitter readings would be erratic. For this reason, a 1004-Hz tone was used in the EOCS as the test tone for loss and as the holding tone for C-notched noise, jitter, and transients. [This is the frequency used in modern transmission maintenance systems.]) The means and standard deviations of the losses are summarized in Table V for the three mileage bands. For comparison, the loss results of the 1969/70 Connection Survey[4] are also shown in the same table. The results from both surveys show that the mean loss increases with mileage, as would be expected from the Via Net Loss (VNL) transmission plan. The VNL design of trunks calls for increasing trunk loss with distance to offset the subjective effect of the increasing echo path delay, until a mileage is reached where an echo suppressor or echo canceler is applied to the trunk. Comparison of the two surveys shows that the mean loss is about the same in both instances, but the standard deviation observed in the EOCS is substantially smaller than in the 1969/70 Connection Survey.

Figure 2 shows "boxplots" of the loss versus airline mileage between the end offices in 100-mile blocks, with the same abscissa as that of Fig. 1. (See Fig. 1 for the number of measurements in each 100-mile block.) For each mileage block on the abscissa, the corresponding boxplot shows the variability of the measurements falling in that mileage block. The upper and lower boundaries of the "box" indicate the 75th and 25th percentiles of the distribution, and the line inside the box indicates the median. Therefore, the height of the box, referred to as the interquartile range, is a measure of variability in the distribution, and the deviation of the median line from the center of the box shows skewness of the distribution. The distance from the median line to the tip of the "whisker" is equal to 1.5 times the interquartile range if there are points falling outside the whisker. If all points fall within the range of 1.5 times the interquartile range on either side of the box, the tip of the lower (or upper) whisker coincides with the minimum (or maximum) value.

Figure 2 shows an overall tendency of increasing loss with mileage of up to about 1200 airline miles, and a decline thereafter. This loss decline can be attributed to the application of echo control devices on trunks, for which the intertoll trunk losses are set to zero. There seems to be a substantial variability in loss for distances between 1200 and 2200 miles. In this mileage region, connections with and without echo control devices are likely to be encountered, which could account for

Table IV—Summary of means and variability measures for analog parameters on end-to-end toll connections

Parameter	Short Mileage Band			Medium Mileage Band			Long Mileage Band			All (Weighted)
	Mean	Standard Deviation Between Pairs Of End Offices	Standard Deviation Within Pairs Of End Offices	Mean	Standard Deviation Between Pairs Of End Offices	Standard Deviation Within Pairs Of End Offices	Mean	Standard Deviation Between Pairs Of End Offices	Standard Deviation Within Pairs Of End Offices	Mean
Loss										
404 Hz	7.86 ± 0.65 dB	1.07	1.37	8.75 ± 0.20	0.93	1.27	9.19 ± 0.28	1.64	1.48	8.10 ± 0.51
1004 Hz	6.53 ± 0.57 dB	0.93	1.34	7.29 ± 0.17	0.80	1.18	7.84 ± 0.21	1.24	1.29	6.75 ± 0.44
2804 Hz	7.88 ± 1.05 dB	1.72	2.00	8.09 ± 0.25	1.17	1.57	8.60 ± 0.25	1.49	1.55	7.97 ± 0.82
EDD										
604 Hz	853 ± 198 μs	316	155	1150 ± 87	393	259	1337 ± 101	571	224	935 ± 155
2804 Hz	599 ± 111 μs	175	149	701 ± 45	203	185	727 ± 39	219	161	624 ± 86
P/AR	87.5 ± 3.0	4.7	4.0	84.5 ± 1.2	5.3	5.5	84.2 ± 1.3	7.8	4.4	86.8 ± 2.3
Delay round trip										
No satellite	9.6 ± 2.0 ms	3.6	2.2	16.0 ± 0.8	3.8	2.4	32.6 ± 1.4	8.6	2.5	12.5 ± 1.6
Only satellite							520.5 ± 3.4	4.9	3.1	

Noise										
C-message	24.6 ± 2.2 dBrnC	3.6	3.4	28.5 ± 0.5	2.2	3.6	31.4 ± 0.5	2.7	2.8	25.7 ± 1.7
C-notch	36.5 ± 1.1 dBrnC	1.8	3.2	37.4 ± 0.3	1.5	2.3	37.9 ± 0.3	1.7	2.1	36.7 ± 0.8
s/n	34.9 ± 1.1 dB	1.7	2.	33.3 ± 0.3	1.3	2.3	32.3 ± 0.2	1.2	2.	34.4 ± 0.8
Flat	43.9 ± 2.6 dBrn	4.2	6.7	44.0 ± 0.5	2.3	6.8	45.4 ± 0.4	2.5	6.4	44.0 ± 2.0
Flat notch	46.2 ± 1.4 dBrn	2.3	5.2	46.0 ± 0.4	1.5	5.1	47.0 ± 0.3	1.9	5.1	46.2 ± 1.1
Noise-to-ground	52.0 ± 3.6 dBrn	6.0	7.9	49.6 ± 0.8	3.5	6.2	50.8 ± 0.6	3.4	5.6	51.6 ± 2.8
Second-order IMD	53.3 ± 1.8 dB	2.8	6.0	52.2 ± 0.6	2.8	5.5	51.6 ± 0.6	3.8	4.8	53.0 ± 1.4
Third-order IMD	53.4 ± 2.5 dB	4.1	5.5	51.0 ± 0.9	4.0	5.9	50.2 ± 0.8	4.9	4.8	52.8 ± 2.0
Jitter										
Amplitude 2–300 Hz	2.8 ± 0.5%	0.8	1.1	3.2 ± 0.1	0.4	1.3	3.6 ± 0.1	0.4	1.5	2.9 ± 0.4
Amplitude 20–300 Hz	2.6 ± 0.4%	0.7	0.8	2.8 ± 0.1	0.3	1.0	3.2 ± 0.1	0.4	1.1	2.7. ± 0.3
Phase 2–300 Hz	5.5 ± 1.9 deg.	3.0	2.2	6.4 ± 0.5	2.1	2.8	7.6 ± 0.4	2.5	2.8	5.8 ± 1.5
Phase 20–300 Hz	3.1 ± 0.5 deg.	0.8	1.2	3.9 ± 0.2	1.1	1.3	4.9 ± 0.2	1.3	1.6	3.3 ± 0.4

Table V—Comparison of 1004-Hz loss from 1982/83 EOCS and 1969/70 Connection Survey

Connection Length (Airline Miles)	1969/70 Survey				EOCS Survey	
	Primary		Secondary		DDD	
	Mean (dB)	Standard Deviation (dB)	Mean (dB)	Standard Deviation (dB)	Mean (dB)	Standard Deviation (dB)
All	6.7 ± 0.6	2.1	6.6 ± 0.3	2.1	6.7 ± 0.4	1.3
0–180	6.5 ± 0.7	2.0	6.4 ± 0.4	2.1	6.5 ± 0.6	1.6
180–720	7.3 ± 0.4	2.3	7.1 ± 0.6	2.1	7.3 ± 0.2	1.4
721–2900	7.7 ± 0.5	2.5	7.4 ± 0.3	2.0	7.8 ± 0.2	1.8

the variability. Above about 2200 miles, the median loss is nearly constant at 6 dB and the variability is small, suggesting that most of the connections in that mileage region have an echo control device. The constant 6-dB loss observed is consistent with a picture of toll connections with one toll-connecting trunk at each end with about 3-dB loss, plus a long, zero-loss intertoll trunk with an echo control device.

Figure 3 gives the Cumulative Distribution Functions (CDFs)* of loss for the three mileage bands. Most of the losses—75 to 90 percent, depending on the mileage category—are greater than 6 dB. This observation is consistent with typical toll connections consisting of the two toll-connecting trunks described above, plus zero to seven (but rarely more than two) intertoll trunks with VNL design losses ranging from 0.5 to 2.9 dB. The losses at the lower tail for the short and medium categories could have come from the connections with no intertoll trunks or with intertoll trunks with negligible VNL loss. The lower tail losses for the long category could have come from the connections with zero-loss intertoll trunks with echo control devices.

Figure 4 shows the CDFs of 1004-Hz loss for customer-premises-to-customer-premises connections. These CDFs were derived by analytically concatenating the 1004-Hz loss of the 1980 Loop Survey[8] to the end office to end office 1004-Hz loss. Figure 5 shows the CDF of 1004-Hz loss for the loops used in the concatenation.

3.2 Frequency response

Frequency response, also referred to as loss-versus-frequency characteristic or attenuation distortion, is a measure of loss variation over the frequency band of a communications channel. It can be measured

* All CDFs in this paper are plotted with an ordinate having the normal probability scale. A normal CDF will show up as a straight line on such a plot, and the vertical scale near the tails of the distribution will be expanded for greater readability.

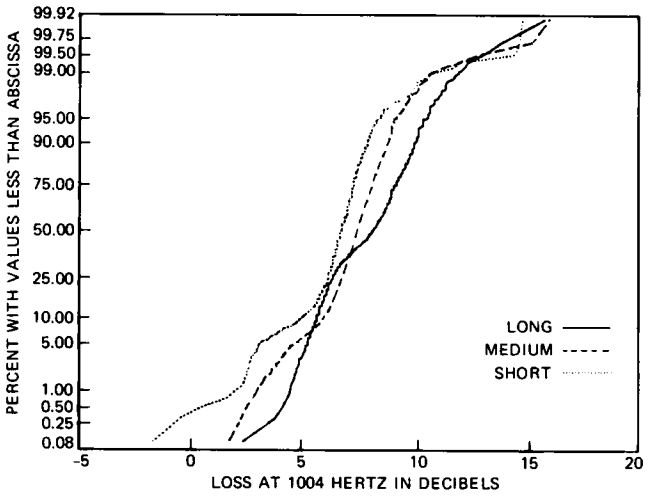

Fig. 3—CDFs of 1004-Hz loss for the short, medium, and long mileage bands.

with sinusoidal test tones or with the 50-percent amplitude-modulated test signal employed to measure the Envelope Delay Distortion (EDD) characteristic. The response of an averaging detector (specified for level measurement by Ref. 1) is the *same* for a sinusoidal tone as for a 50-percent amplitude-modulated signal.

To characterize frequency response, loss was measured from 204 to 3504 Hz. Losses at 204, 254, and 3504 Hz were obtained from a sinusoidal test tone, while the losses at the other frequencies were

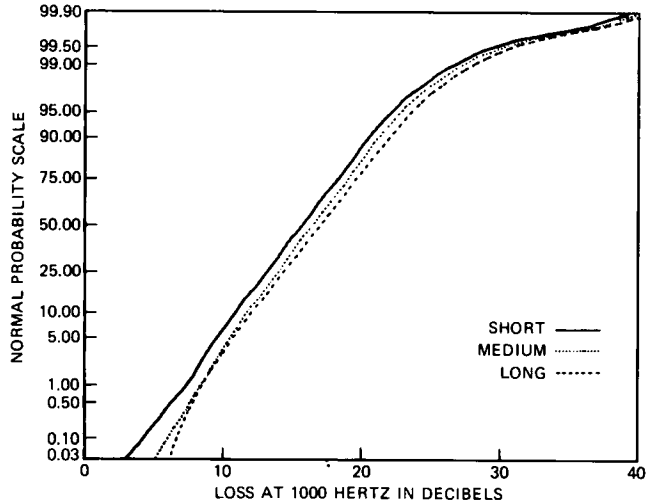

Fig. 4—CDFs of customer premises-to-customer premises 1004-Hz loss.

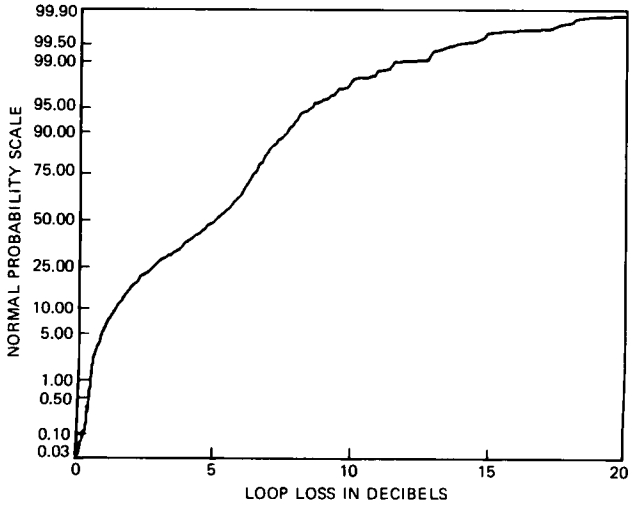

Fig. 5—CDF of 1004-Hz loss on customer loops.

obtained from level measurements of the envelope delay distortion test signal.

Tables VI through VIII show the means, standard deviations, and selected percentiles of loss versus frequency relative to 1004 Hz for

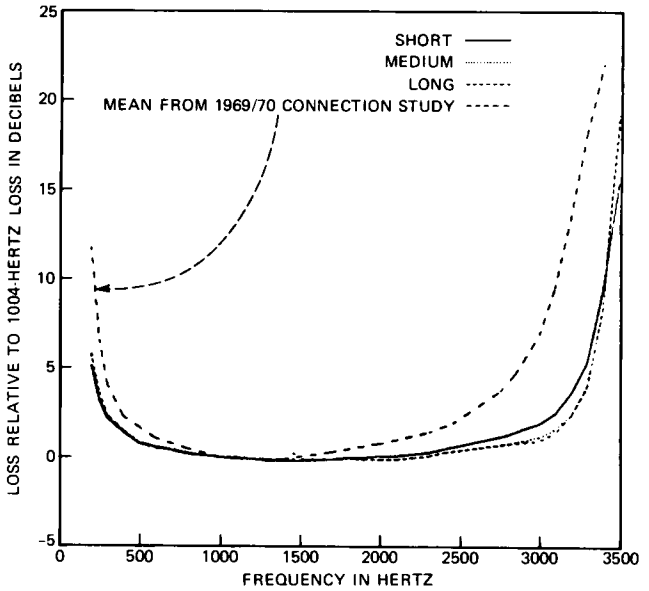

Fig. 6—Man attenuation distortion relative to 1004 Hz for short, medium, and long mileage bands.

Table VI—Attenuation distortion relative to 1004 Hz: short connections

Frequency in Hz	Mean	Standard Deviation	Quantiles				
			1%	10%	50%	90%	99%
204	5.1 ± 2.9	2.8	2.0	2.5	3.8	10.0	13.2
254	3.3 ± 1.9	1.9	0.9	1.4	2.8	6.4	7.4
304	1.8 ± 1.1	1.2	0.2	0.5	1.6	3.7	4.7
404	1.1 ± 0.4	0.7	−0.8	0.4	1.1	2.0	2.9
504	0.7 ± 0.2	0.4	0.1	0.2	0.7	1.3	2.0
604	0.4 ± 0.1	0.3	−0.6	0.0	0.4	0.9	1.3
704	0.3 ± 0.0	0.3	−0.4	0.0	0.3	0.6	1.2
804	0.2 ± 0.1	0.2	−0.5	0.0	0.2	0.4	0.6
904	0.1 ± 0.0	0.3	−1.2	0.0	0.1	0.2	1.1
1004	0.0 ± 0.0	0.0	0.0	0.0	0.0	0.0	0.0
1104	−0.1 ± 0.1	0.4	−2.3	−0.3	−0.1	0.1	1.3
1204	−0.1 ± 0.1	0.2	−0.6	−0.4	−0.1	0.0	0.4
1304	−0.2 ± 0.2	0.3	−1.7	−0.5	−0.1	0.1	0.7
1404	−0.2 ± 0.2	0.4	−1.2	−0.6	−0.2	0.1	0.6
1504	−0.2 ± 0.2	0.4	−1.3	−0.6	−0.1	0.2	0.8
1604	−0.1 ± 0.1	0.4	−1.2	−0.5	−0.1	0.2	1.0
1704	0.0 ± 0.1	0.4	−1.3	−0.4	0.0	0.3	1.0
1804	0.0 ± 0.2	0.4	−1.5	−0.3	0.0	0.4	1.3
1904	0.1 ± 0.3	0.4	−1.2	−0.3	0.0	0.6	1.2
2004	0.1 ± 0.5	0.6	−1.4	−0.4	−0.1	0.9	1.5
2104	0.2 ± 0.7	0.7	−1.4	−0.4	−0.1	1.0	2.5
2204	0.3 ± 0.8	0.9	−1.4	−0.4	−0.1	1.4	3.3
2304	0.4 ± 0.9	1.0	−1.2	−0.4	0.0	1.9	3.4
2404	0.6 ± 1.1	1.1	−0.9	−0.3	0.1	2.3	3.5
2804	1.7 ± 2.7	2.6	−0.6	−0.1	0.3	5.8	10.0
2904	2.0 ± 3.2	3.0	−0.7	−0.2	0.4	6.8	11.4
3004	2.3 ± 3.5	3.3	−0.6	−0.2	0.5	7.3	12.3
3104	3.1 ± 4.2	4.0	−0.4	0.0	0.9	8.8	15.3
3204	4.1 ± 4.9	4.6	0.2	0.5	1.5	11.5	18.2
3304	5.3 ± 5.3	5.0	1.1	1.5	2.3	13.8	17.7
3404	7.4 ± 4.6	4.2	3.2	5.0	5.9	14.4	23.8
3504	16.5 ± 7.5	6.0	4.2	5.2	19.2	21.2	22.2

short, medium, and long connections. In the tables, the measured frequencies above 304 Hz are at intervals of 10 Hz, except 2504, 2604, and 2704 Hz were omitted. Because of the wide use of the 2600-Hz idle-circuit tone for signaling, the presence of a signal with energy concentrated near 2600 Hz could inadvertently cause disconnection.

Figure 6 presents the mean losses of Tables VI through VIII as a function of frequency for short, medium, and long connections. The losses between 2404 and 2804 Hz (not measured in the EOCS) were obtained by linear interpolation.

For comparison, the mean losses relative to 1004 Hz from the 1969/70 Connection Survey are also shown in Fig. 6. As we can see in the figure, the mean frequency response has improved since that survey. This improvement can be attributed to the increasing use of T-carrier to replace voice-frequency cable facilities in the toll-connecting portion

Table VII—Attenuation distortion relative to 1004 Hz: medium connections

Frequency in Hz	Mean	Standard Deviation	Quantiles				
			1%	10%	50%	90%	99%
204	5.7 ± 0.3	2.1	2.4	3.6	5.3	8.3	13.1
254	3.4 ± 0.2	1.4	1.0	1.9	3.2	5.2	8.2
304	2.1 ± 0.1	1.0	0.3	1.0	2.0	3.2	5.5
404	1.4 ± 0.1	0.7	0.0	0.7	1.4	2.2	3.3
504	0.9 ± 0.1	0.5	−0.1	0.4	0.9	1.5	2.1
604	0.6 ± 0.0	0.3	0.0	0.3	0.6	1.1	1.6
704	0.5 ± 0.0	0.3	−0.1	0.2	0.5	0.8	1.3
804	0.3 ± 0.0	0.2	−0.1	0.1	0.3	0.5	0.9
904	0.1 ± 0.0	0.1	−0.2	0.0	0.1	0.2	0.5
1004	0.0 ± 0.0	0.0	0.0	0.0	0.0	0.0	0.0
1104	0.0 ± 0.0	0.1	−0.4	−0.2	0.0	0.1	0.2
1204	−0.1 ± 0.0	0.2	−0.6	−0.3	−0.1	0.1	0.3
1304	−0.2 ± 0.0	0.2	−0.8	−0.4	−0.1	0.1	0.3
1404	−0.2 ± 0.0	0.2	−0.9	−0.5	−0.2	0.0	0.3
1504	−0.2 ± 0.0	0.3	−0.9	−0.5	−0.2	0.1	0.3
1604	−0.2 ± 0.0	0.3	−1.0	−0.5	−0.2	0.1	0.4
1704	−0.1 ± 0.0	0.4	−0.9	−0.5	−0.1	0.2	0.6
1804	−0.1 ± 0.0	0.3	−1.0	−0.5	−0.1	0.3	0.7
1904	−0.1 ± 0.0	0.4	−1.0	−0.5	−0.1	0.3	0.8
2004	−0.1 ± 0.1	0.6	−1.1	−0.5	−0.1	0.4	1.0
2104	−0.1 ± 0.1	0.6	−1.1	−0.6	−0.1	0.5	1.1
2204	0.0 ± 0.1	0.6	−1.1	−0.5	0.0	0.6	1.4
2304	0.1 ± 0.1	0.7	−1.0	−0.5	0.0	0.7	1.7
2404	0.3 ± 0.1	0.9	−1.0	−0.4	0.2	0.9	2.7
2804	0.8 ± 0.2	1.2	−0.7	−0.1	0.6	2.0	5.4
2904	1.0 ± 0.2	1.1	−0.6	−0.0	0.7	2.5	4.4
3004	1.2 ± 0.3	1.3	−0.6	0.0	0.8	3.3	5.4
3104	1.6 ± 0.3	1.6	−0.5	0.2	1.1	4.5	6.8
3204	2.3 ± 0.4	2.0	0.2	0.8	1.8	5.9	8.9
3304	3.8 ± 0.5	2.5	1.3	1.8	3.0	8.4	12.5
3404	7.5 ± 0.5	2.5	4.1	5.4	6.9	10.1	16.4
3504	19.2 ± 0.5	2.5	12.7	16.0	19.3	22.2	24.3

of the network. This is corroborated by the observation that digital channel banks of the D3 and D4 type, which provide the interface between the analog voice-frequency signals and the 1.544-Mb/s digital bit stream of the T-carrier system, have a frequency response similar to that of the current survey, shown in Fig. 6.

The gain slope at 404 or 2804 Hz is defined as the loss at that frequency minus the loss at 1004 Hz. Figure 7 plots the CDFs of the larger of the gain slopes (per connection) at 404 and 2804 Hz for short, medium, and long connections. Figures 8 through 10 show the CDFs of loss difference for the frequency pairs of 2804 and 604 Hz, 2404 and 804 Hz, and 2104 and 1304 Hz, respectively. As the figures show, there is little mileage dependence for these loss differences except for a tendency for short connections (possibly on VF cables) to have somewhat higher loss difference.

Table VIII—Attenuation distortion relative to 1004 Hz: long connections

Frequency in Hz	Mean	Standard Deviation	Quantiles				
			1%	10%	50%	90%	99%
204	5.9 ± 0.4	2.8	2.2	3.1	5.0	10.1	14.1
254	3.7 ± 0.3	2.0	0.7	1.7	3.2	6.6	10.4
304	2.1 ± 0.2	1.5	−0.2	0.5	1.8	4.2	7.0
404	1.4 ± 0.1	0.9	−0.2	0.4	1.2	2.5	4.3
504	0.8 ± 0.1	0.5	−0.2	0.2	0.8	1.5	2.5
604	0.5 ± 0.0	0.4	−0.2	0.0	0.5	1.0	1.6
704	0.4 ± 0.0	0.3	−0.3	0.0	0.4	0.8	1.3
804	0.2 ± 0.0	0.2	−0.2	0.0	0.2	0.5	0.9
904	0.1 ± 0.0	0.1	−0.2	0.0	0.1	0.2	0.5
1004	0.0 ± 0.0	0.0	0.0	0.0	0.0	0.0	0.0
1104	0.0 ± 0.0	0.2	−0.5	−0.2	0.0	0.1	0.3
1204	−0.1 ± 0.0	0.2	−0.7	−0.3	−0.1	0.1	0.4
1304	−0.1 ± 0.0	0.2	−0.8	−0.4	−0.1	0.1	0.4
1404	−0.1 ± 0.0	0.4	−0.9	−0.4	−0.1	0.1	0.4
1504	−0.1 ± 0.0	0.4	−1.0	−0.5	−0.1	0.1	0.5
1604	−0.1 ± 0.0	0.4	−1.1	−0.5	−0.1	0.2	0.6
1704	−0.1 ± 0.0	0.4	−1.2	−0.5	0.0	0.3	0.7
1804	0.0 ± 0.0	0.5	−1.2	−0.5	0.0	0.3	0.8
1904	−0.1 ± 0.0	0.5	−1.2	−0.5	−0.1	0.4	0.9
2004	−0.1 ± 0.0	0.5	−1.3	−0.6	−0.1	0.4	1.1
2104	−0.1 ± 0.1	0.6	−1.3	−0.6	−0.1	0.4	1.3
2204	0.0 ± 0.1	0.6	−1.2	−0.6	−0.1	0.5	1.6
2304	0.1 ± 0.1	0.7	−1.1	−0.5	0.0	0.7	1.8
2404	0.3 ± 0.1	0.8	−1.0	−0.4	0.2	1.0	2.5
2804	0.8 ± 0.1	1.1	−0.8	−0.1	0.6	1.9	4.7
2904	0.9 ± 0.2	1.2	−0.8	−0.2	0.6	2.3	5.0
3004	1.0 ± 0.2	1.3	−0.7	−0.1	0.7	2.6	5.7
3104	1.4 ± 0.2	1.6	−0.6	0.1	1.0	3.2	7.4
3204	2.2 ± 0.3	1.9	0.0	0.6	1.7	4.2	10.2
3304	3.6 ± 0.4	2.4	1.0	1.6	2.9	6.2	13.4
3404	7.5 ± 0.3	2.1	4.2	5.4	6.9	10.4	14.3
3504	19.2 ± 0.6	2.8	9.5	16.4	19.5	22.0	25.4

Figure 11 shows the same type of information that is in Fig. 6 for customer-premises-to-customer-premises connections, obtained by concatenating the frequency response of the loops to the frequency response of the EOCS connections. The concatenation was done, using the 1980 Loop Survey data, using the same technique described in the previous section. The mean frequency response of the loops (two per connection) used in the concatenation is also shown in Fig. 11. Loop effects clearly dominate trunk effects in end-to-end frequency response.

3.3 Envelope delay distortion

Envelope delay is defined as the negative of the derivative of the phase of the received signal with respect to frequency. *Envelope Delay Distortion* (EDD) at a given frequency is defined as the difference

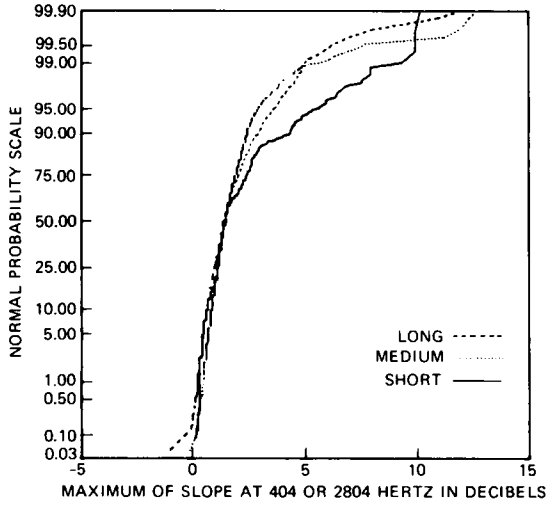

Fig. 7—CDFs of the maxium of the two gain slopes at 404 and 2804 Hz relative to 1004 Hz for short, medium, and long mileage bands.

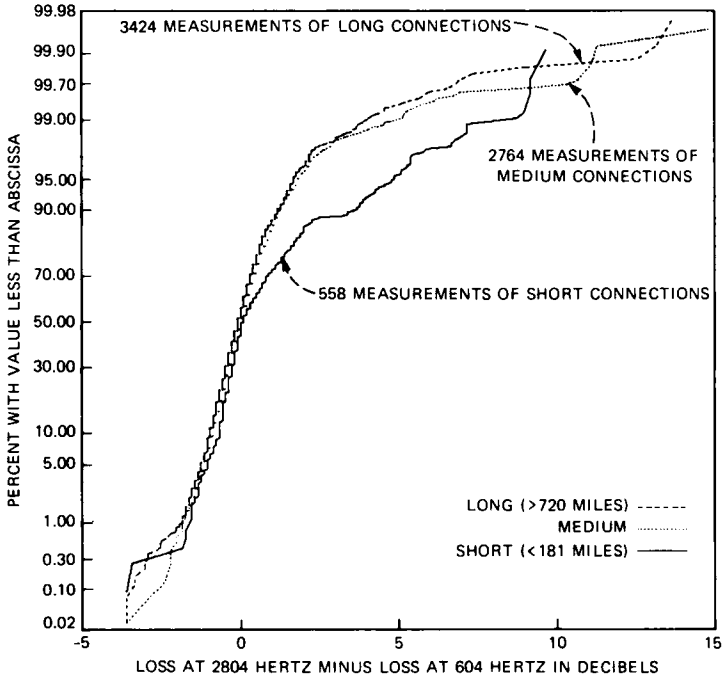

Fig. 8—CDFs of loss at 2804 Hz minus loss at 604 Hz for short, medium, and long mileage bands.

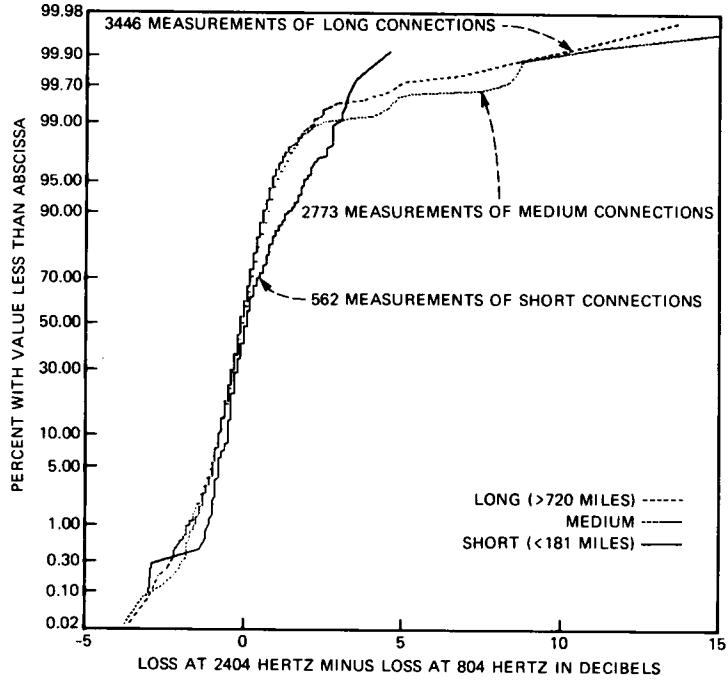

Fig. 9—CDFs of loss at 2404 Hz minus loss at 804 Hz for short, medium, and long mileage bands.

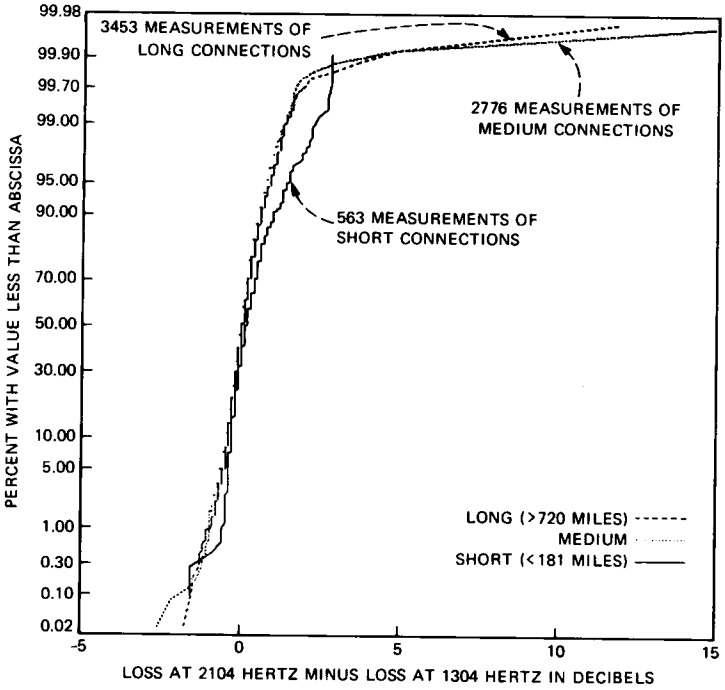

Fig. 10—CDFs of loss at 2104 Hz minus loss at 1304 Hz for short, medium, and long mileage bands.

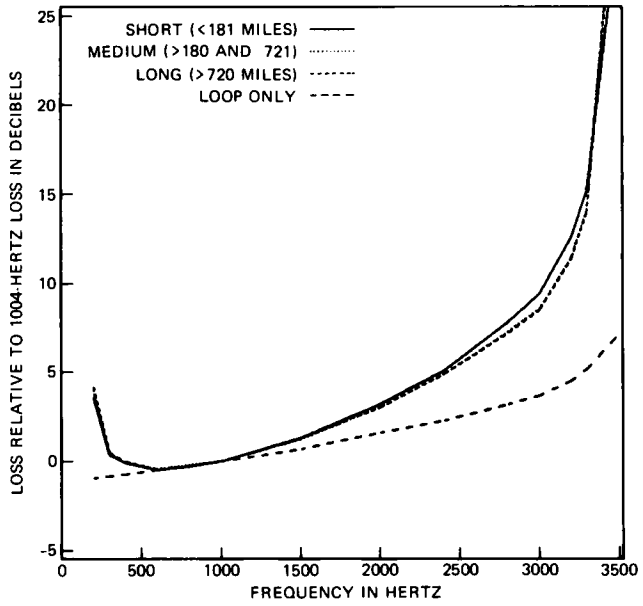

Fig. 11—Mean customer-premises-to-customer-premises attenuation distortion relative to 1004 Hz obtained by analytically concatenating the EOCS result and the 1980 Loop Survey result. The 1980 Loop Survey result is also shown.

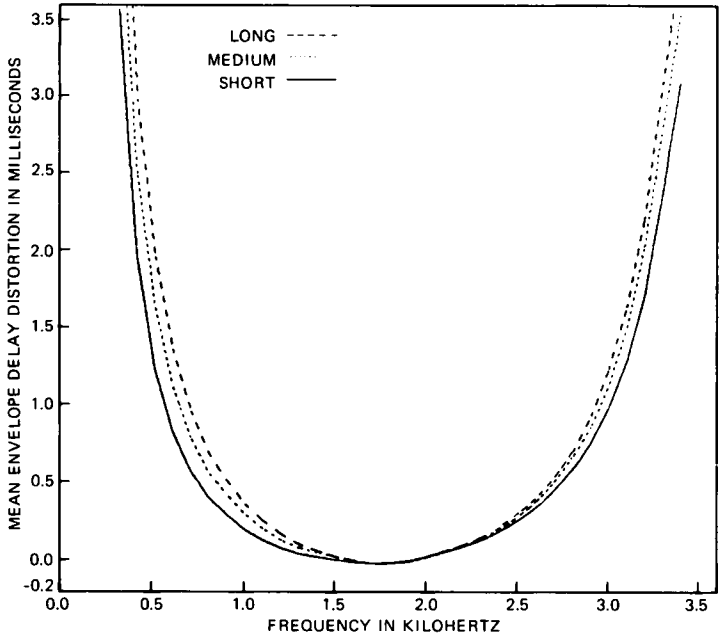

Fig. 12—Mean EDD for short, medium, and long mileage bands.

between the envelope delay at that frequency and the envelope delay at the reference frequency (usually between 1600 and 1800 Hz), where the delay is near the minimum value. The reference frequency used in the EOCS was 1704 Hz.

The test signal used for envelope delay distortion measurement in the United States, which is also used in the EOCS, is a voiceband carrier frequency amplitude modulated (50 percent) by an 83-1/3 Hz tone. A return reference path is required to establish the phase reference so that the phase of the transmitted 83-1/3 Hz envelope can be compared to the phase of the received 83-1/3 Hz envelope. Since the frequency aperture of the modulated test signal remains fixed at twice the 83-1/3 Hz as the carrier frequency of the modulated test signal is varied, the recovered phase changes give estimates of the slope of the phase-versus-frequency curve (EDD). The more desirable direct measurement of phase versus frequency is not made because of the possibility of frequency shift on the facility.

The effect of a nonlinear phase-versus-frequency characteristic (as measured by EDD) on a data signal is such that the different frequency components of the signal have different transit times, which results in distortion in the received signal. The effect of EDD on data signals can be compensated by employing equalizers in the data set receiver. The effectiveness of an equalizer depends on the equalization scheme used—fixed or adaptive—and the complexity (e.g., number of taps) in the equalizer.

Tables IX through XI show the means, standard deviations, and selected percentiles of EDD versus frequency for the short, medium, and long connections. As in the 1969/70 Connection Survey, 1704 Hz was selected as the reference frequency for EDD measurements in the EOCS. Figure 12 shows the mean EDD versus frequency for the short, medium, and long mileage categories. Although not shown in Fig. 12, the mean EDD for the 1969/70 Connection Survey is practically coincident with the short mileage category.

Figure 13 shows the CDFs of the larger of the EDD values at 604 and 2804 Hz for the short, medium, and long mileage categories. Figure 14 is a scatter plot of EDD at 604 Hz compared to that at 2804 Hz, which shows that there is little dependence (correlation coefficient of 0.53) between the EDDs at the two frequencies. Figures 15 and 16 show that there is even less correlation between EDD and loss at these frequencies (correlation coefficient of 0.32 at 604 Hz and 0.37 at 2804 Hz).

3.4 Peak-to-average ratio

Peak-to-Average Ratio (P/AR) measurements are made on a straightaway basis with a transmitter and a receiver attached at

Table IX—Envelope delay distortion relative to 1704 Hz (all statistics expressed in μs): short connections

Frequency in Hz	Mean	Standard Deviation	Quantiles				
			1%	25%	50%	75%	99%
304	3580	1221	1103	3029	3324	4226	6725
404	1959	684	492	1695	1876	2185	3885
504	1242	460	108	1114	1209	1365	2492
604	839	334	15	748	819	922	1749
704	577	258	−71	506	556	637	1278
804	409	190	−35	356	398	456	922
904	298	148	−71	254	293	333	700
1004	205	121	−137	161	201	239	526
1104	136	92	−125	95	128	165	375
1204	87	79	−121	44	77	111	273
1304	54	53	−67	20	48	76	199
1404	36	47	−119	12	32	52	145
1504	20	37	−150	5	19	32	91
1604	7	36	−85	−1	7	14	66
1704	0	0	0	0	0	0	0
1804	6	32	−78	−2	4	11	69
1904	21	32	−92	12	21	29	105
2004	50	39	−58	35	49	61	146
2104	82	47	−39	63	84	98	216
2204	119	57	−27	92	122	142	259
2304	166	65	8	136	165	197	329
2404	220	88	36	177	212	261	493
2804	609	217	102	541	584	727	1021
2904	787	248	136	704	766	909	1243
3004	1017	312	159	949	1008	1176	1567
3104	1312	405	198	1248	1307	1466	1967
3204	1734	551	226	1651	1744	1951	2606
3304	2410	772	253	2304	2470	2625	3739
3404	3132	1102	295	3062	3256	3443	5189

opposite ends of a connection. The transmitter generates a precisely controlled complex waveform of known peak-to-average ratio. The energy in the waveform is dispersed in time by the bandwidth reduction and envelope delay distortion encountered on the connection in a way that may be directly related to intersymbol interference (eye closing) of data signals.[9] The P/AR receiver measures the peak and full-wave average values of the waveform and displays their ratio on a zero-suppressed scale. A P/AR value of 100 suggests no pulse degradation.

The P/AR signal is largely insensitive to noise, phase jitter, and intermodulation distortion, and is unaffected by frequency shift or transient phenomena. P/AR does not produce unambiguous diagnostic information, so there are no externally published requirements for P/AR. Since P/AR ignores transients, P/AR readings cannot predict data set error performance on connections where the transients dominate data set performance. P/AR values may be the same for different EDD shapes occurring on real connections, and with the addition of

Table X—Envelope delay distortion relative to 1704 Hz (all statistics expressed in μs): medium connections

Frequency in Hz	Mean	Standard Deviation	Quantiles				
			1%	25%	50%	75%	99%
304	4290	1292	2787	3261	3755	4951	7819
404	2497	936	1579	1830	2101	2959	5465
504	1633	631	1016	1191	1340	2009	3706
604	1129	457	661	809	912	1403	2654
704	794	339	418	557	638	977	1904
804	574	249	275	401	456	735	1371
904	427	189	190	299	339	553	1034
1004	306	152	109	207	240	402	775
1104	208	112	34	132	161	279	543
1204	135	97	−18	77	106	183	378
1304	86	69	−40	46	70	122	265
1404	61	78	−31	30	48	83	182
1504	37	56	−29	18	30	50	115
1604	16	46	−31	6	12	22	55
1704	0	0	0	0	0	0	0
1804	1	71	−45	−9	−1	7	35
1904	15	27	−53	3	16	26	79
2004	45	46	−45	26	44	59	153
2104	85	65	−33	59	80	98	252
2204	126	77	−17	93	115	143	353
2304	175	109	3	130	155	197	458
2404	235	153	24	174	204	261	585
2804	692	265	264	557	596	768	1588
2904	888	308	383	723	772	977	1950
3004	1156	377	551	955	1007	1261	2437
3104	1523	481	757	1268	1321	1646	3175
3204	2048	638	1079	1697	1784	2178	4242
3304	2828	843	1694	2352	2507	2964	5558
3404	3585	877	2277	3093	3285	3724	6320

sophisticated EDD adaptive equalizers in data sets, the utility of P/AR has diminished. P/AR serves as a quick straightaway measure of the relative bandwidth reduction and EDD on a significant percentage of connections.

Figure 17 shows that there is almost no relationship between P/AR and connection mileage except that there are almost no short connections with a P/AR rating below 70. The figure also shows rare P/AR values above 100, which usually suggest connections where the loss at the band edges is less than that at the center of the band. Such connections increase the peak value of the received P/AR signal relative to the average value. Such a connection in tandem with a "normal" connection (which has higher loss at the band edges) will improve the P/AR value over that of the normal connection alone.

Figures 18 through 20 are scatter plots of P/AR versus the maximum of EDDs at 604 and 2804 Hz, which are test frequencies for network performance objectives. These frequencies have no special relationship

Table XI—Envelope delay distortion relative to 1704 Hz (all statistics expressed in μs): long connections

Frequency in Hz	Mean	Standard Deviation	Quantiles				
			1%	25%	50%	75%	99%
304	5032	1427	2928	3616	4881	6055	8194
404	2997	1245	1633	2028	2398	3624	6714
504	1959	881	1031	1280	1498	2356	4534
604	1366	643	680	875	1035	1640	3222
704	966	469	438	610	729	1165	2292
804	698	350	280	435	521	853	1685
904	515	266	184	317	386	641	1255
1004	371	201	105	224	275	470	921
1104	258	146	53	153	191	328	659
1204	173	112	16	101	133	217	459
1304	111	75	−12	64	89	143	305
1404	73	72	−26	40	57	96	216
1504	42	62	−38	20	32	56	134
1604	16	29	−31	4	12	23	66
1704	0	0	0	0	0	0	0
1804	2	28	−49	−7	2	9	39
1904	20	29	−64	6	21	31	80
2004	51	46	−65	32	51	66	141
2104	90	59	−72	67	88	108	219
2204	132	73	−66	102	125	154	304
2304	181	115	−54	140	166	206	407
2404	239	129	−16	186	214	275	515
2804	726	275	285	567	604	807	1573
2904	954	347	412	745	797	1051	2073
3004	1258	452	588	976	1039	1393	2765
3104	1659	586	836	1277	1374	1857	3657
3204	2224	761	1182	1721	1852	2509	4788
3304	3105	989	1750	2457	2623	3502	6249
3404	3912	1018	2260	3247	3447	4496	6804

to the P/AR signal. These figures show that there is a reasonably strong correlation (particularly for longer connection mileages) between EDD at 604 or 2804 Hz (whichever is higher) and P/AR, in that when EDD* is higher, P/AR is lower. The two straight lines (labeled 1 and 2) in these figures are the regression lines of P/AR versus EDD and EDD versus P/AR. The degree to which line 1 differs from line 2 is directly related to the coefficient of correlation: the two lines would coincide if P/AR and EDD were perfectly correlated.

The ellipses of concentration shown in these figures have five parameters: two of them determine the center position; one, the angular orientation; and two, the lengths of the major/minor axes. These parameters were determined so that a uniform, elliptical mass of data points would have the same means, standard deviations, and

* EDD in the remainder of this subsection refers to the maximum (per connection) of EDDs at 604 and 2804 Hz.

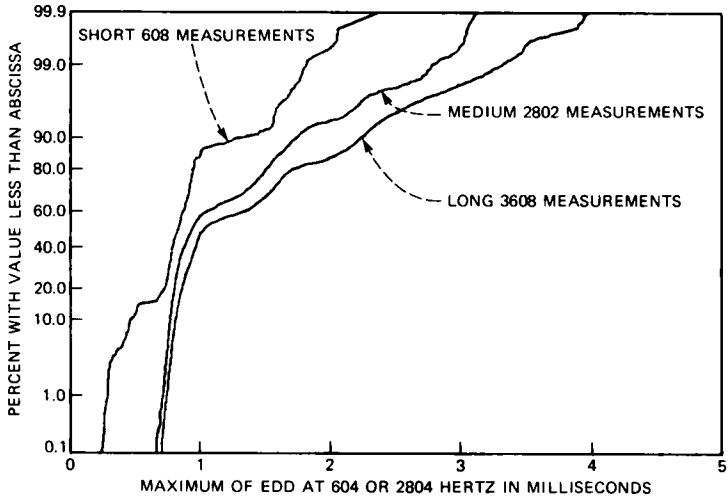

Fig. 13—CDFs of the maximum of the two EDDs at 604 and 2804 Hz relative to 1704 Hz for short, medium, and long mileage bands.

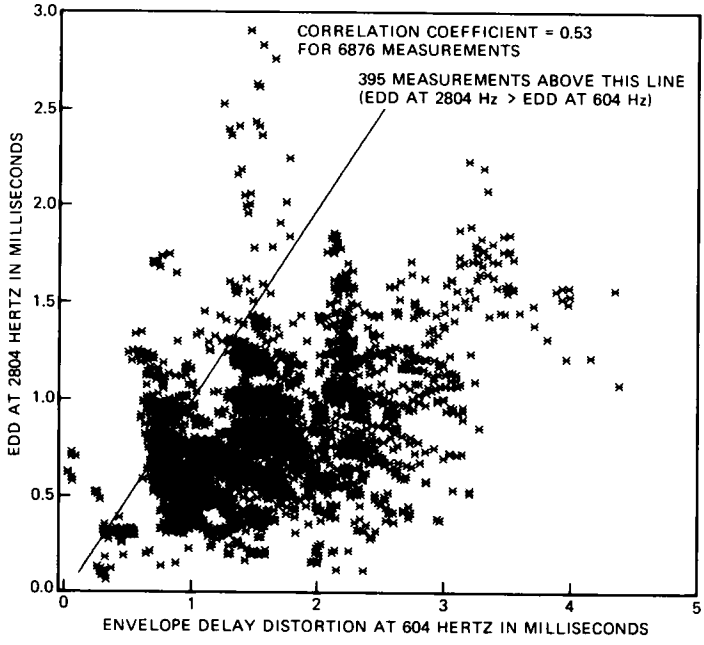

Fig. 14—EDD (relative to 1704 Hz) at 2804 Hz versus EDD (relative to 1704 Hz) at 604 Hz.

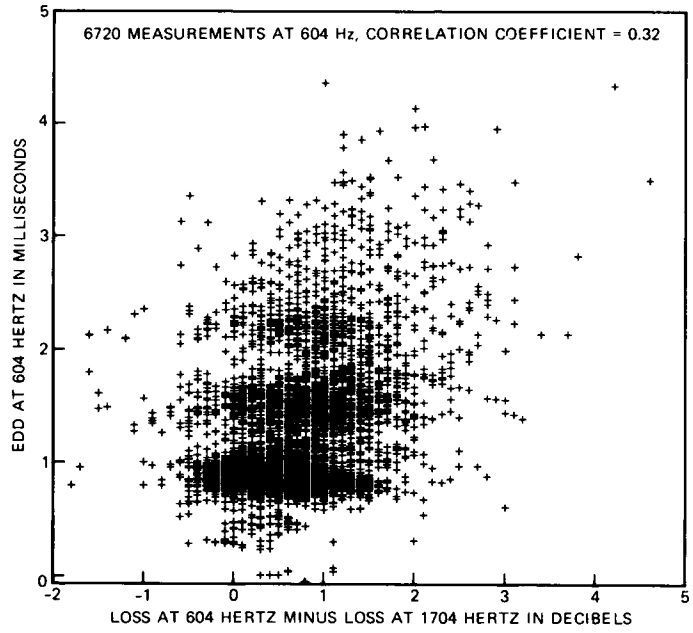

Fig. 15—EDD versus attenuation distortion at 604 Hz, both relative to 1704 Hz.

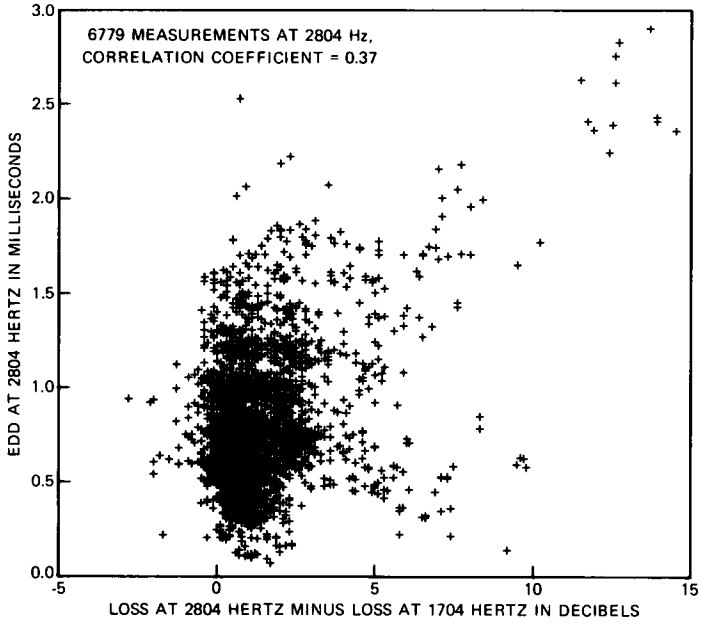

Fig. 16—EDD versus attenuation distortion at 2804 Hz, both relative to 1704 Hz.

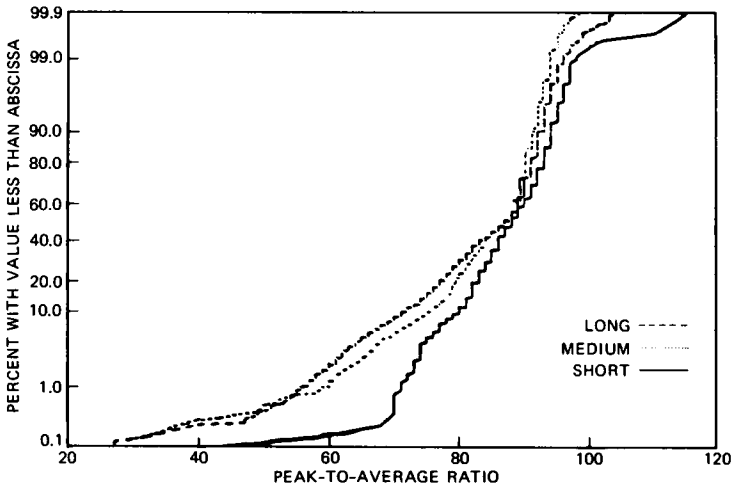

Fig. 17—CDFs of P/AR for short, medium, and long mileage bands.

correlation coefficient as the original data. The ellipse of concentration has two horizontal and two vertical tangents passing through the points where, respectively, line 1 and line 2 intersect the ellipse. The distance between the two horizontal tangents is equal to four times the standard deviation of P/AR. Similarly, the distance between the

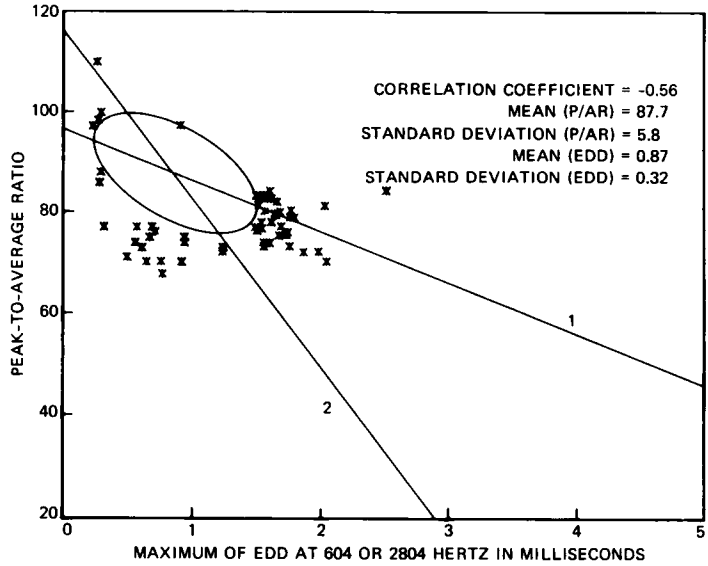

Fig. 18—P/AR versus the maximum of the EDDs at 604 and 2804 Hz for the short mileage band (563 measurements). Eighty-six percent of the points fall within the ellipse and are not plotted.

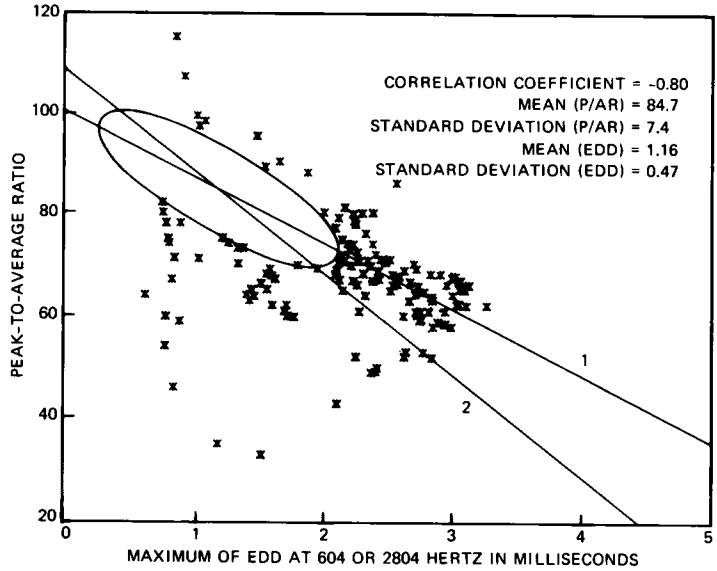

Fig. 19—P/AR versus the maximum of the EDDs at 604 and 2804 Hz for the medium mileage band (2586 measurements). Ninety percent of the points fall within the ellipse and are not plotted.

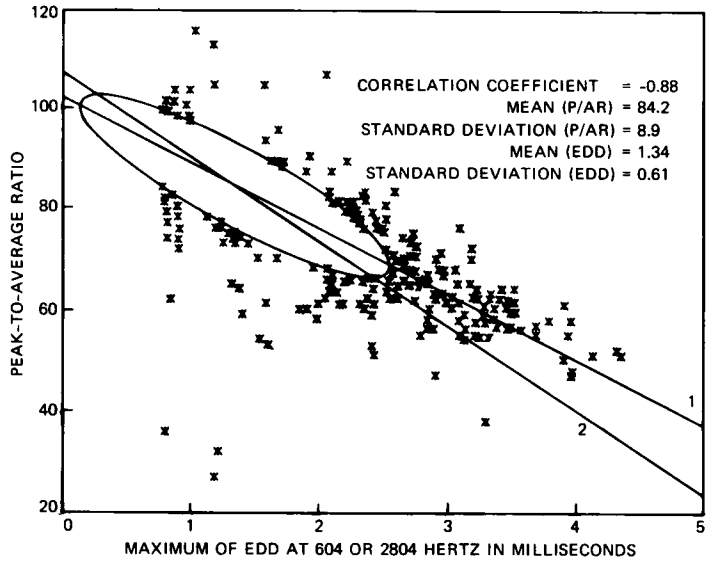

Fig. 20—P/AR versus the maximum of the EDDs at 604 and 2804 Hz for the long mileage band (3218 measurements). Ninety percent of the points fall within the ellipse and are not plotted.

two vertical tangents is equal to four times the standard deviation of EDD. Almost 90 percent of the measurements fall within the ellipses.

3.5 Propagation delay

Round-trip propagation delay measurements were made in the EOCS by using full-duplex 1200-b/s data sets (to be described in 3.13) under the control of the microprocessor in the ASPEN RTU. An error was introduced in a continuous repetition of a 511-bit pseudorandom word transmitted by the near-end RTU microprocessor bit error rate generator to the low-band modulator of the full-duplex 1200-b/s data set. When the far-end RTU microprocessor recognized the error from the low-band demodulator of its 1200-b/s data set, it immediately introduced an error in the continuous repetition of the same 511-bit pseudorandom word being transmitted back to the near end by the high-band 1200-b/s data set modulator. When the near-end RTU microprocessor recognized the forced error, it corrected for the known (fixed) processing delay to get a first estimate of round-trip propagation delay. This sequence was repeated nine more times to obtain enough valid measurements to reject those affected by random errors on the connection.

Figure 21 shows boxplots of round-trip propagation delay versus mileage (with the same abscissa as that of Fig. 1), except for the 52 measurements taken on satellite connections.* Round-trip delay measurements on these satellite connections ranged from 508 to 539 ms. The variability in round-trip delay for the same end office building pairs can be attributed to alternate trunk facilities as well as alternate routing. Figure 22 shows CDFs of round-trip delay for the three mileage bands. In Figs. 21 and 22, measurements on satellite connections were excluded from these CDFs with the 52 measurements on satellites excluded. The boxplots and the CDFs show a strong dependence of round-trip delay on airline mileage.

3.6 Message circuit noise and signal-to-C-notched noise ratio

Message circuit noise was measured both with and without a 1004-Hz holding tone, with both the C-message and 3-kHz flat weighting filters, as Ref. 1 specifies. The C-message filter weighting characteristic was derived in 1957 from tests made with subjects assessing the interfering effects of single frequency interference as heard over an ordinary telephone handset. This weighting is also appropriate for high-speed data transmission because most high-speed modems concentrate their transmitted energy in approximately the same band of sensitivity as the C-message filter. The ac power-line hum at 60 Hz

* Propagation delay is the only parameter in this paper for which measurements on satellite connections are treated separately.

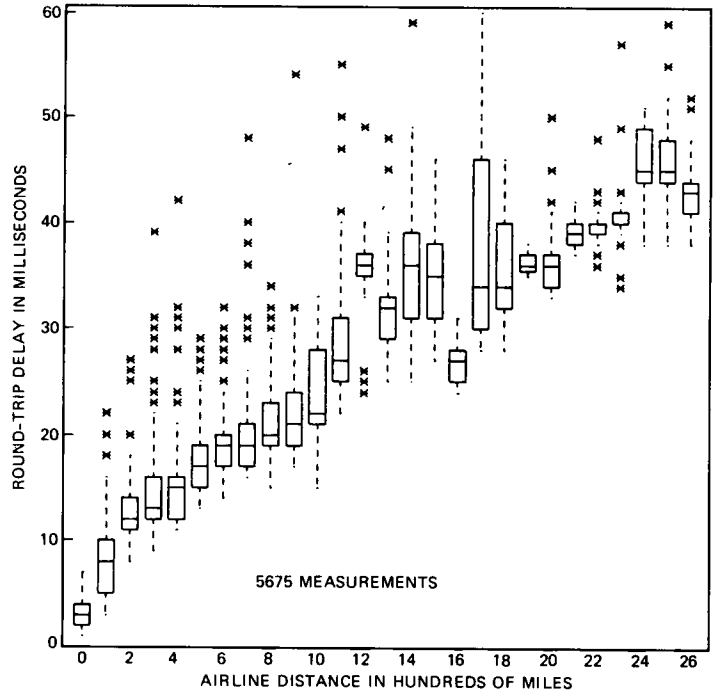

Fig. 21—Round-trip propagation delay versus connection airline mileage in 100-mile blocks.

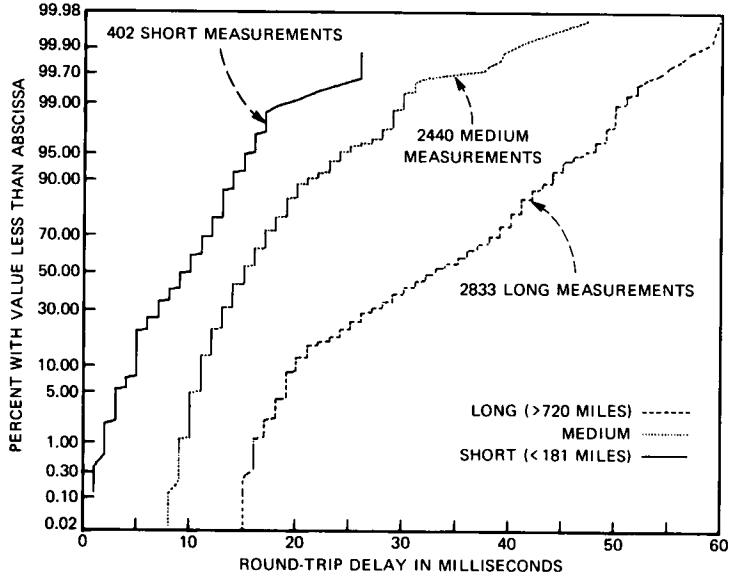

Fig. 22—The cumulative distributions of round-trip propagation delay.

(and odd harmonics of 60 Hz), frequently encountered in the loop plant, is attenuated by the C-message filter but is included in the noise measurements made with the 3-kHz flat filter. All noise measurements were reported as they were measured, without corrections for losses in the office in which the measurements were made, which permits direct comparison with the 1969/70 Connection Survey,[4] and concatenation with the loop plant.[8]

If a connection has facilities with digital channel banks or compandors, noise on that connection can be substantially different, depending on whether it is measured with or without a holding tone. For data transmission, therefore, C-notched noise is more relevant than C-message noise. C-notched noise is obtained by filtering out the 1004-Hz holding tone with a deep (50-dB) notch filter and then measuring C-message noise. Signal-to-C-notched-noise ratio (s/n) is the ratio of the received 1004-Hz holding tone power to the C-notched noise power.

The s/n is an essential performance measure for digital channel banks. As Fig. 23 shows, digital channel banks have an approximately logarithmic (μ255) encoder/decoder that maintains a nearly constant s/n over a reasonable range of signal levels. Because most of the connections measured in the EOCS have at least one T-carrier link, the s/n results from the EOCS are dominated by this characteristic. This can be observed in the figures that follow.

Figure 24 shows the CDFs of s/n for the three mileage bands. The CDFs confirm mileage dependence of s/n, particularly in the region of "good" s/n or the upper tails. Comparison of these CDFs with similar CDFs obtained from the 1969/70 Connection Survey shows that the variability of s/n on short connections has been reduced substantially since the last survey. This tighter s/n distribution for short connections in the EOCS is caused by the introduction of T-carrier systems in the network since the 1969/70 Connection Survey. The same comparison suggests that the percentage of short connections with s/n better than 40 dB—the s/n ceiling for digital channel banks observed in Fig. 23—was greater in the 1969/70 Connection Survey than in the EOCS. However, this s/n degradation, which can also be attributed to T-carrier facilities, is largely inconsequential to the performance of data sets in the region where it occurs, i.e., the upper tail of the CDF. Listeners are usually unable to discern differences in s/n ratios above 40 dB.

Figure 25 shows the Probability Density Functions (PDFs) of s/n for the three mileage bands. The PDF for the short mileage category shows bimodality, whereas the PDFs for the medium and long mileage categories are unimodal. The two peaks for the short category occur at 34 and 38 dB. The peak at 38 dB is consistent with the noise expected on a connection with one T-carrier system with one digital

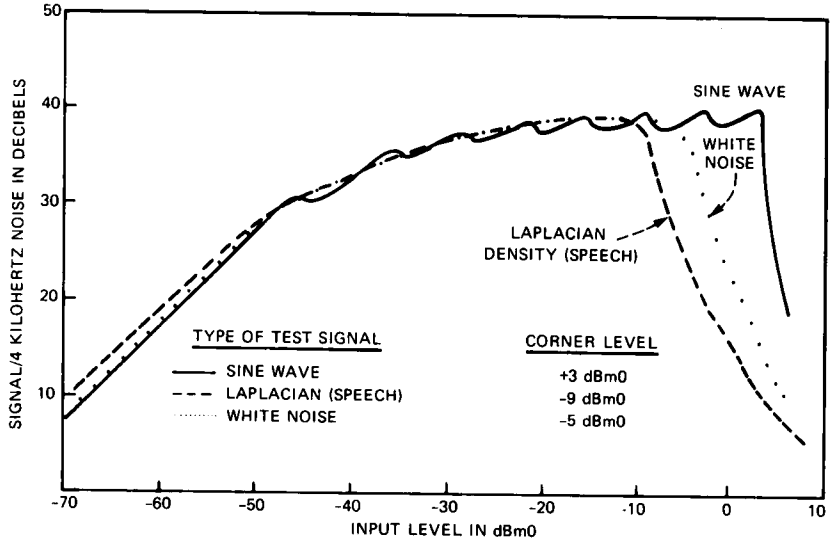

Fig. 23—Signal-to-distortion performance of 8-bit μ=255 coder-decoder (15-segment approximation, 8 segments +, 8 −).

channel bank at each end—one analog-to-digital (A/D) and one digital-to-analog (D/A) conversion, i.e., an end-to-end digital connection or an analog connection with exactly one digital facility or digital switch; see Fig. 23. The lower peak is consistent with occurrences of two digital links in tandem.

Figure 26 shows a scatter plot of C-notched noise versus C-message

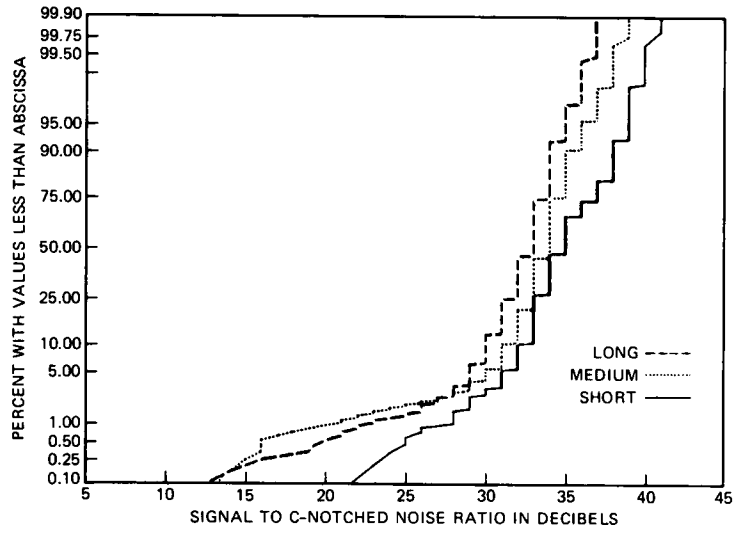

Fig. 24—CDFs of signal-to-C-notched-noise ratio for short, medium, and long mileage bands.

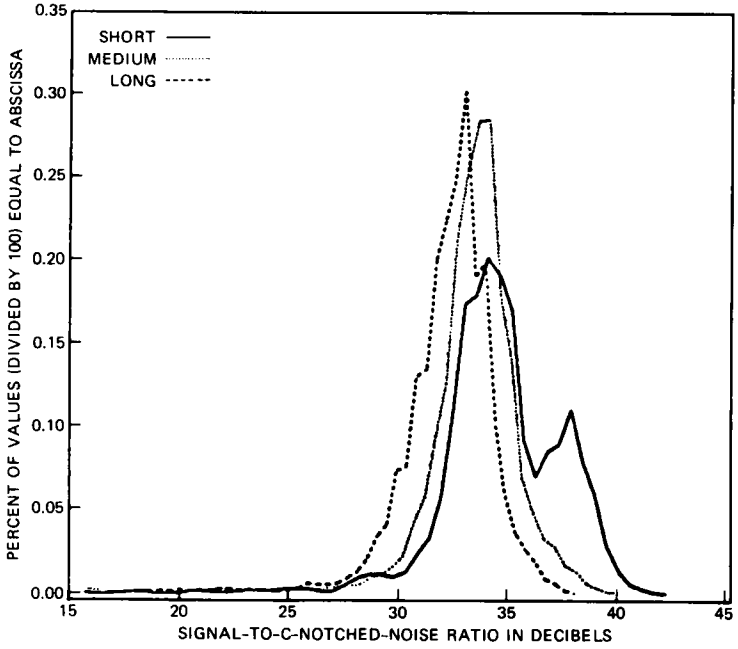

Fig. 25—PDFs of signal-to-C-notched-noise ratio for short, medium, and long mileage bands.

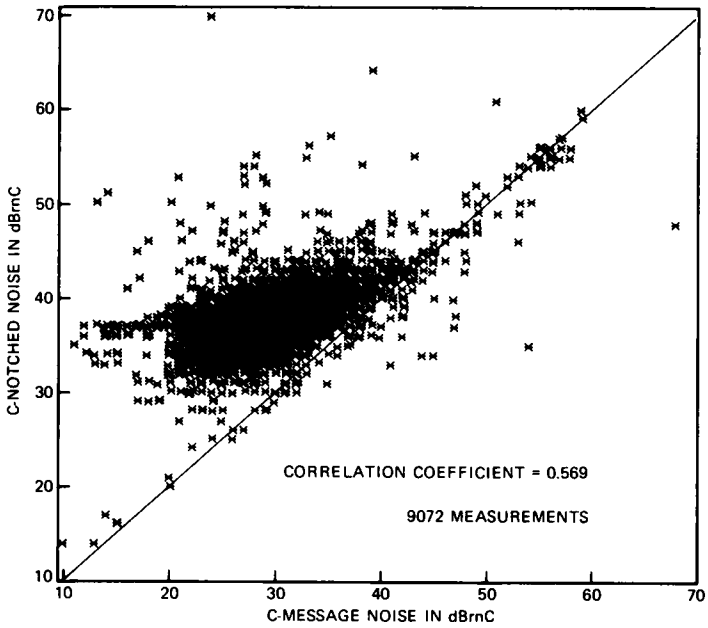

Fig. 26—C-notched noise versus C-message noise.

noise. Also shown in the figure is a straight line on which C-notched noise is equal to C-message noise. The large cluster of points above the line, corresponding to the connections with higher C-notched noise than C-message noise, show the effects of compandors, quantizing noise, and harmonic distortion on the holding tone. The points scattered far above the line may correspond to the connections where bad coders were encountered or where the C-notched noise measurements were affected by impulse noise. The points along the line represent the connections where the tone had no effect on noise. Small deviations from the line can be expected, considering possible time variation of noise between the two types of noise measurement. The points scattered far below the line indicate the possible effects of impulse noise during the C-message noise measurements.

Figure 27 shows the CDFs of C-message noise for the three mileage bands. The mileage dependence of C-message noise can be observed in the figure, as would be expected for the analog carrier facilities normally encountered on longer trunks. The airline-mileage effect on the C-message noise can also be seen on the boxplots of Fig. 28 (see Fig. 2 for the explanation of the abscissa).

Figure 29 presents the CDFs of C-notched noise for the three mileage bands. Mileage dependence is less apparent with C-notched noise than with C-message noise. In particular, Fig. 29 shows virtually no difference in the CDF of C-notched noise between the medium and long mileage categories. It appears that most connections measured for these mileage categories had T-carrier facilities on the toll-connecting trunks, one at each end, which dominated the connection C-notched noise. The dominance of the toll connecting trunk noise reduces the dependence of noise on connection mileage for the longer connections. Digital switches in tandem with T-carrier links do not degrade the C-notched noise.

It appears that the C-notched noise measurements for the short mileage category consist of measurements from two groups of connections, as evidenced by the bimodality of the s/n PDF in Fig. 25: one group containing two pairs of digital channel banks, and the other containing one pair of digital channel banks. As Fig. 29 shows, the upper half of the CDF for the short mileage category is almost the same as the CDFs for the other two categories, suggesting that it is made up of the measurements from the connections with two pairs of digital channel banks. The lower half of the CDF for the short mileage category, however, is significantly different from those for the other two mileage categories, suggesting that the measurements are from the connections with one pair of digital channel or from Voice Frequency (VF) cable.

Figure 30 shows the CDFs of the 3-kHz flat noise for the three

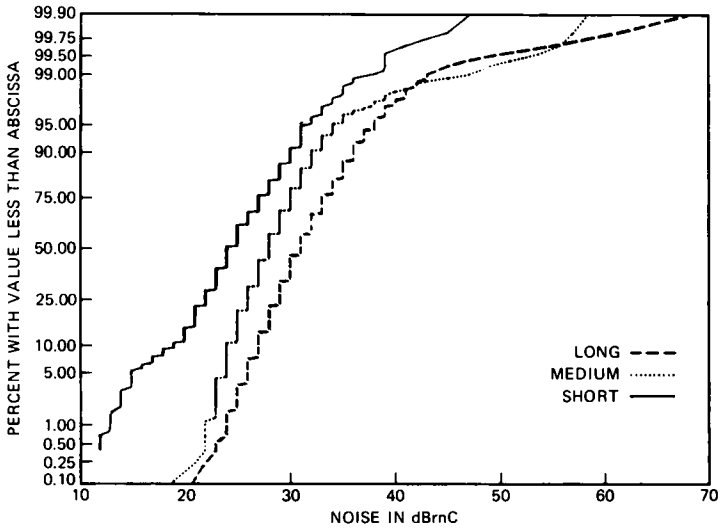

Fig. 27—CDFs of C-message noise for short, medium, and long mileage bands.

mileage bands. As we can see in the figure, the 3-kHz flat noise shows almost no dependence on mileage and is much higher than the C-message noise. This shows that this type of noise is dominated by sources outside the range of the C-message filter, primarily multiples

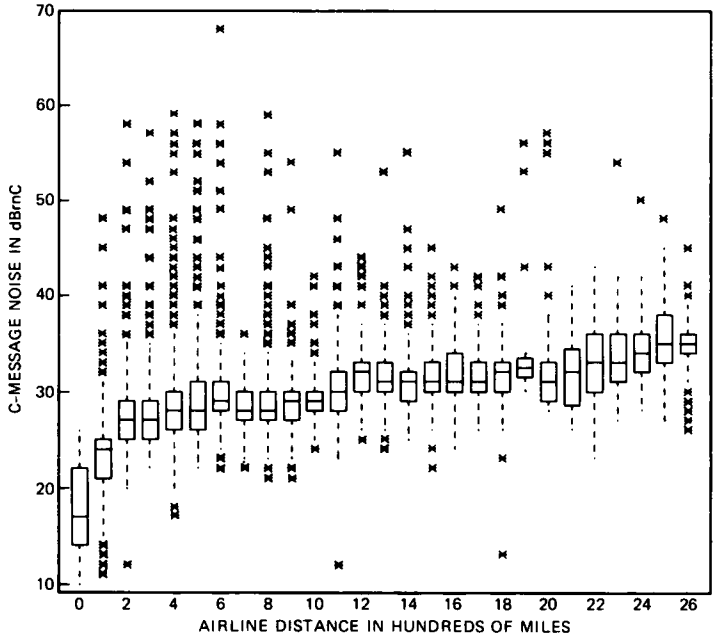

Fig. 28—C-message noise versus airline mileage in 100-mile blocks.

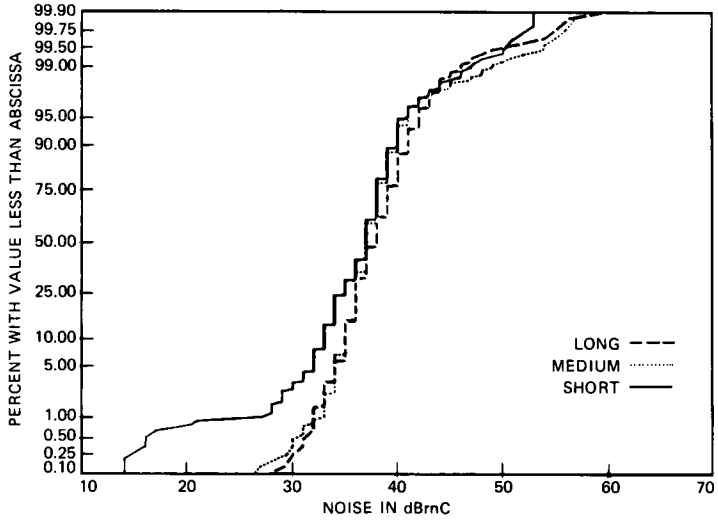

Fig. 29—CDFs of C-notched noise for short, medium, and long mileage bands.

of 60 Hz from the end office line-circuit battery feed. The same remarks made for the 3-kHz flat noise hold for the 3-kHz flat notched noise. Figure 31 shows the CDFs of the 3-kHz flat notched noise for the three mileage bands.

Figure 32 shows the CDFs of the 3-kHz flat noise-to-ground per environment of the end office: urban, suburban, and rural. An urban

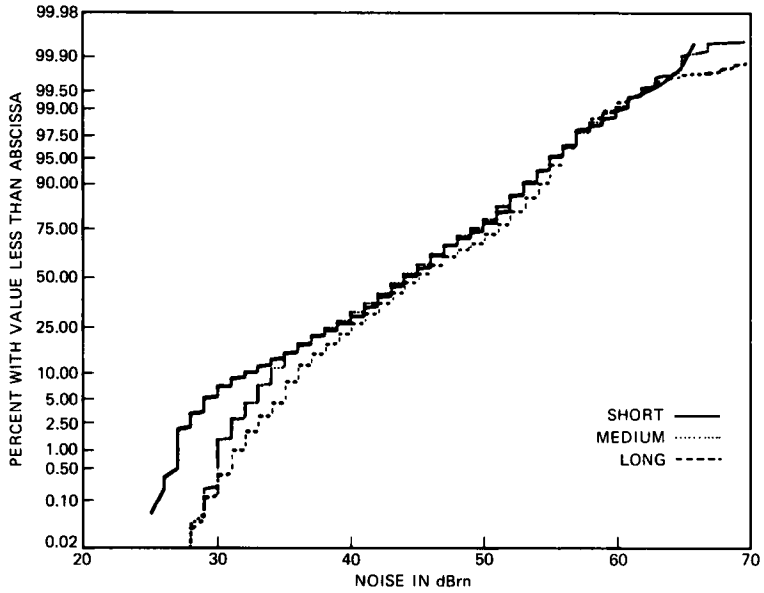

Fig. 30—CDFs of 3-kHz flat noise for short, medium, and long mileage bands.

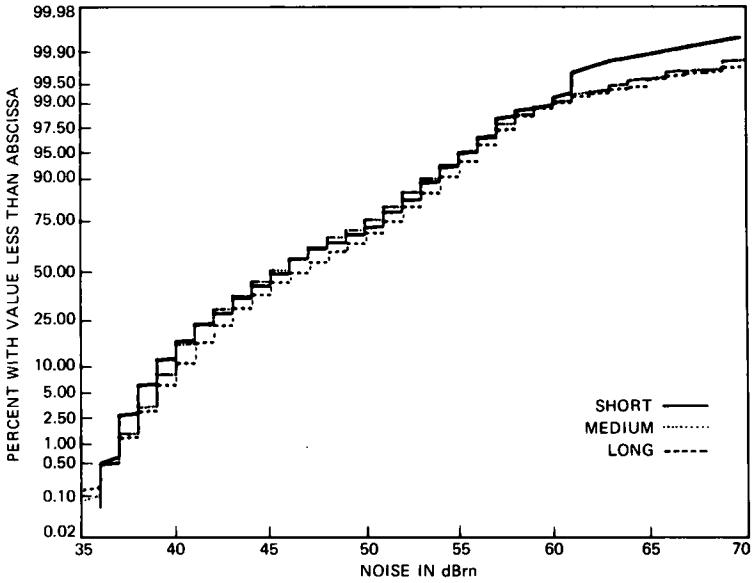

Fig. 31—CDFs of 3-kHz flat-notched noise for short, medium, and long mileage bands.

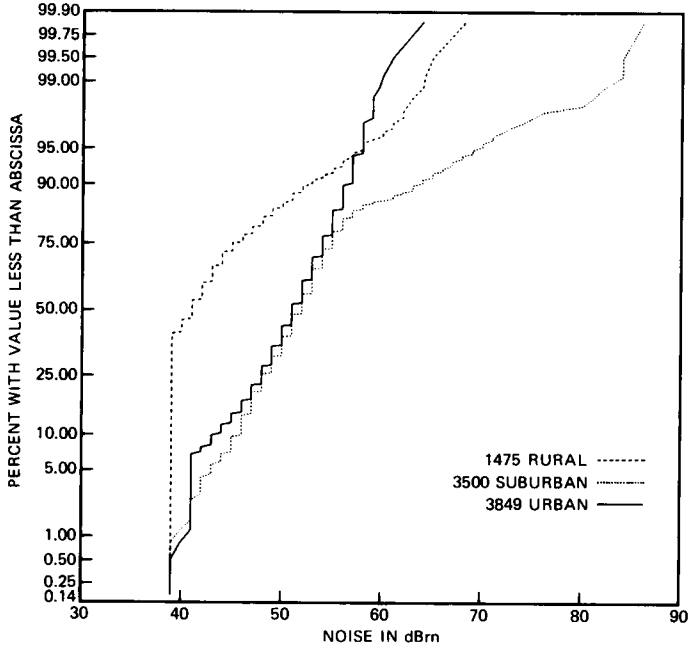

Fig. 32—CDFs of 3-kHz flat noise-to-ground in central offices classified as rural, suburban, and urban.

end office was defined in Ref. 8 as one serving more than 20,000 assigned pairs; a rural end office as one serving fewer than 5000 assigned pairs; and a suburban end office as one serving between 5000 and 20,000 assigned pairs. The bottom of the measuring range for the test equipment for noise-to-ground was 40 dBrn, so measured values below this value were conservatively estimated at 39 dBrn, causing the truncation in the CDFs at that value. It should be recalled that no loops were connected for EOCS measurements. These measurements confirmed that the medians for 3-kHz flat noise-to-ground for trunks in the central office with no loops connected were well below the median contribution for trunks connected to the loop plant[8] (by 12-dB for urban, 20 dB for suburban, and 40 dB for rural central offices).

Figure 33 shows the CDFs of C-message noise on customer-premises-to-customer-premises connections. The calculated customer C-message noise power of a connection was obtained by power-summing the noise power of the connection measured at the end office attenuated by the loss of the loop, and the C-message noise on the loop (customer end). Figure 33 was obtained by analytically concatenating (using discrete convolution techniques) the loop noise from the 1980 Loop Survey to the end office to end office C-messsage noise attenuated by the loop loss. Also included in the same figure for comparison is the CDF of the end office to end office C-message noise for the EOCS medium connection length category. The distribution of the C-message noise can be seen to improve with the addition of the loop. The contribution of the loop loss (which attenuates the noise from the end office) is apparently more important than the effect of the noise on the loop.

Figure 34 shows the CDF of C-message weighted metallic noise for Bell System loops from the 1980 Loop Survey used in the concatenation for Figure 33. (The CDF of 1004-Hz loss for the Bell System loops used in the concatenation appears on Fig. 5.)

3.7 Intermodulation distortion

In the past, a harmonic distortion measurement was used to characterize nonlinearities by applying a single tone to the connection and measuring the received power at the second and third harmonics of the test frequency with a selective detector. However, this type of measurements did not properly characterize nonlinearities as they affected data transmission. The harmonics of the sine wave could cancel one another on connections with multiple nonlinearities, and the PDF of noise-like high-speed data signals is markedly different from that of a single tone.

In the EOCS, nonlinearities were evaluated by an intermodulation distortion measurement using the four-tone method.[1] The four-tone

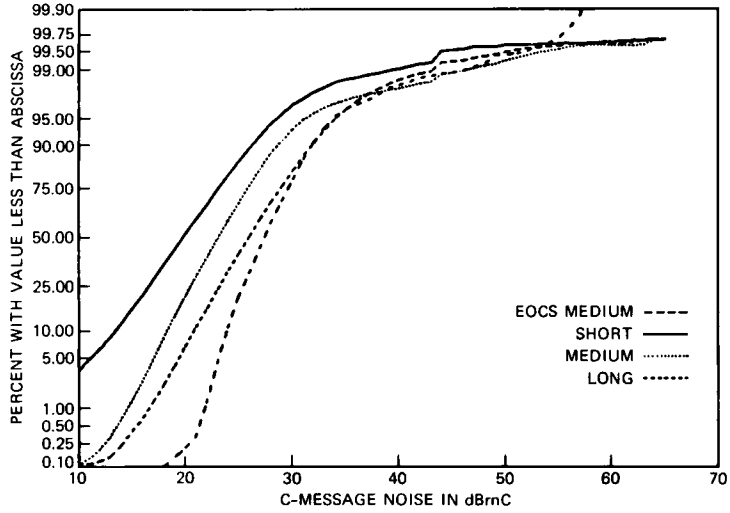

Fig. 33—CDFs of the customer-premises-to-customer-premises C-message noise for short, medium, and long mileage bands.

method is not subject to the cancellation effect, and the PDF of its test signal is a much better approximation to the PDF of a high-speed data modem signal than is a sinusoidal (one-tone) test signal.

The intermodulation distortion measured with the four-tone test signal may contain components caused by background or quantizing

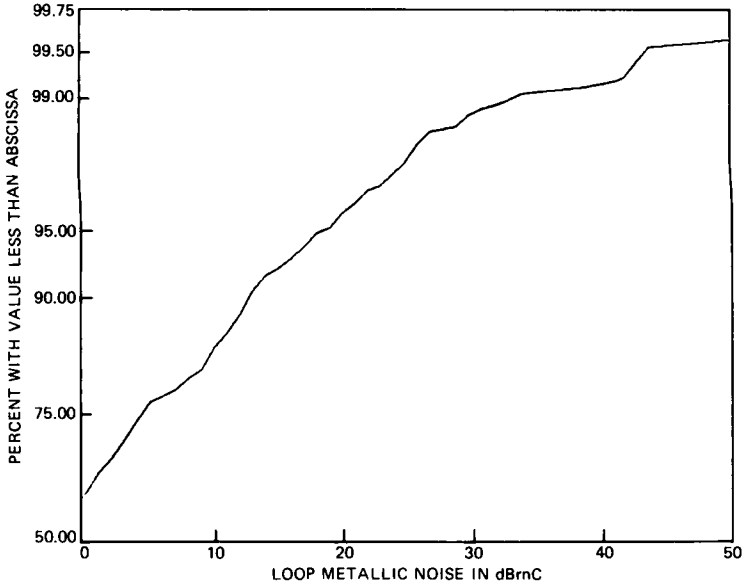

Fig. 34—CDF of C-message weighted metallic noise on customer loops.

noise. To correct for this, the noise component was measured by removing two of the four tones and measuring the energy in the narrow bands where the four-tone intermodulation distortion would fall. The corrected intermodulation distortion was then calculated by power subtraction of the noise component from the original measurement, as outlined in Ref. 1. (For example, if the power measured with four tones was 1 dB larger than that measured with two tones, the true intermodulation distortion would be 7 dB below the value measured with four tones. If the levels measured with four tones and with two tones were the same, the conservative value of 8 dB was subtracted from the four-tone intermodulation distortion measurement.)

Figures 35 and 36 show the CDFs of second- and third-order intermodulation distortion for the three mileage bands. The abscissa shows intermodulation distortion expressed as a signal-to-distortion ratio in decibels, and thus higher values on the abscissa represent better performance. As we can see in the figure, there is little dependence on mileage, particularly for the medium and long mileage categories. Intermodulation distortion on connections in these mileage categories could have been contributed mostly by central office equipment, such as multiplexors, whose appearance is only weakly correlated with mileage.

The scatter plot of third-order versus second-order intermodulation distortion of Fig. 37 shows moderate correlation between the two parameters.

3.8 Phase and amplitude jitter

Phase jitter is the deviation or "jitter" of zero-crossings of a 1004-Hz tone from their nominal position in time. Phase jitter was measured by comparing the average phase of the signal (determined by a phase-locked loop) and the instantaneous phase of the received signal. The normal bandwidth for the measurement of (demodulated) phase jitter is 20 to 300 Hz. In the EOCS, phase jitter was measured in two bands: 20 to 300 Hz and 2 to 300 Hz. The bandwidth of the phase jitter detector in the transmission test set used in the EOCS extends below the recommended 4-Hz corner of Ref. 1.

Amplitude jitter is the deviation or "jitter" of the peak of a 1004-Hz tone from its nominal value. Amplitude jitter was measured with the same two frequency bands as the phase jitter, and the phase and amplitude jitter circuits used the same post-detection filter and peak detector.

Figures 38 and 39 show the CDFs of phase jitter for the 20- to 300-Hz band and for the 2- to 300-Hz band, respectively, for the three mileage bands. The figures show dependence of phase jitter on mileage.

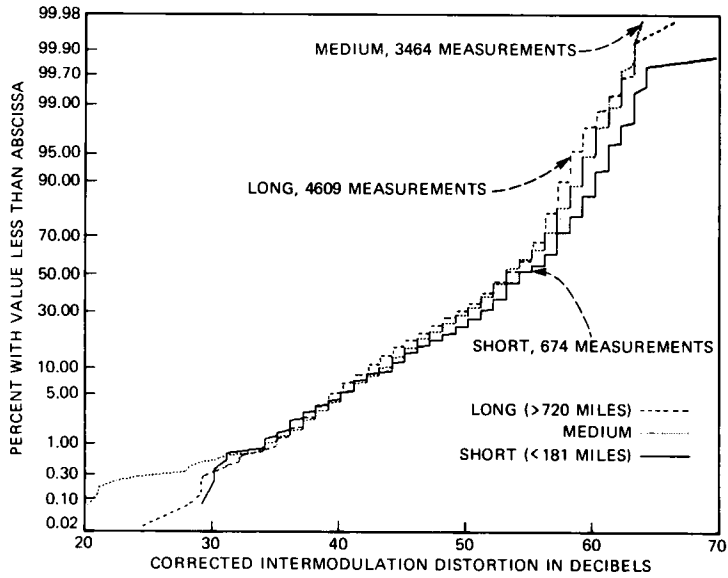

Fig. 35—CDFs of second-order intermodulation distortion for short, medium, and long mileage bands.

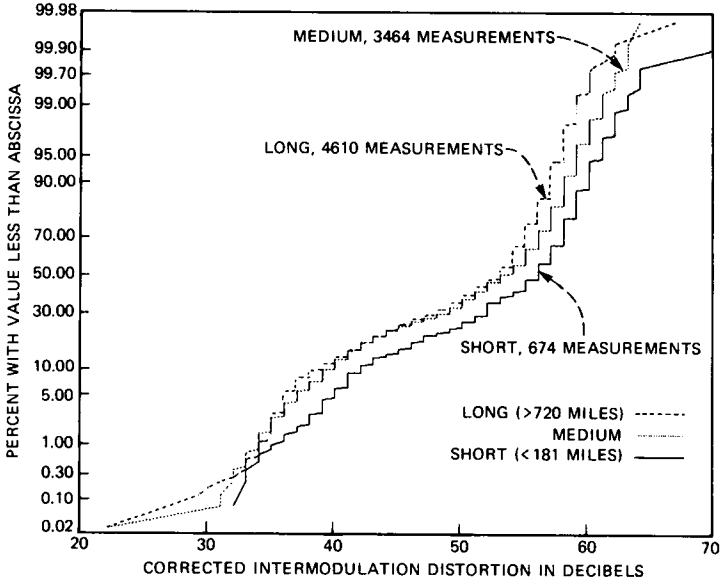

Fig. 36—CDFs of third-order intermodulation distortion for short, medium, and long mileage bands.

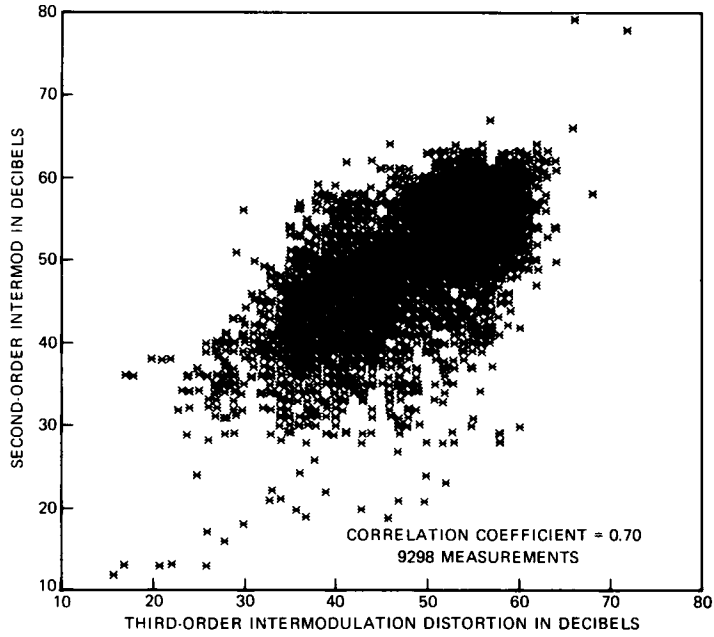

Fig. 37—Second-order versus third-order intermodulation distortion.

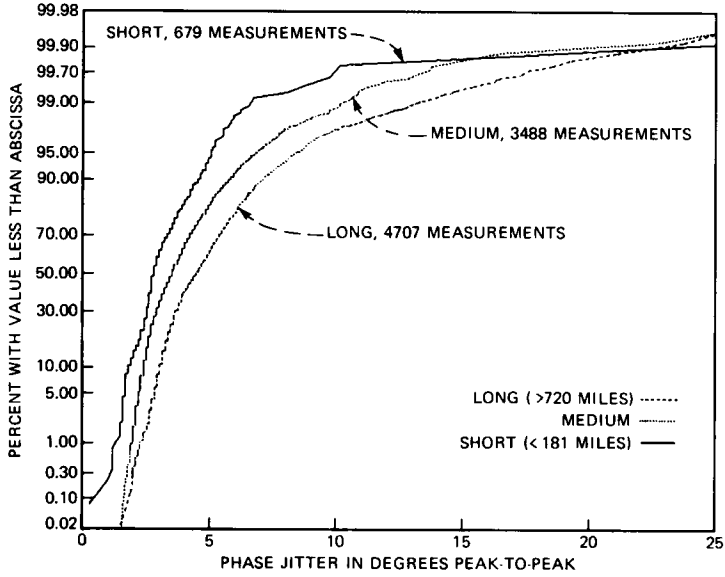

Fig. 38—CDFs of 20- to 300-Hz phase jitter for short, medium, and long mileage bands.

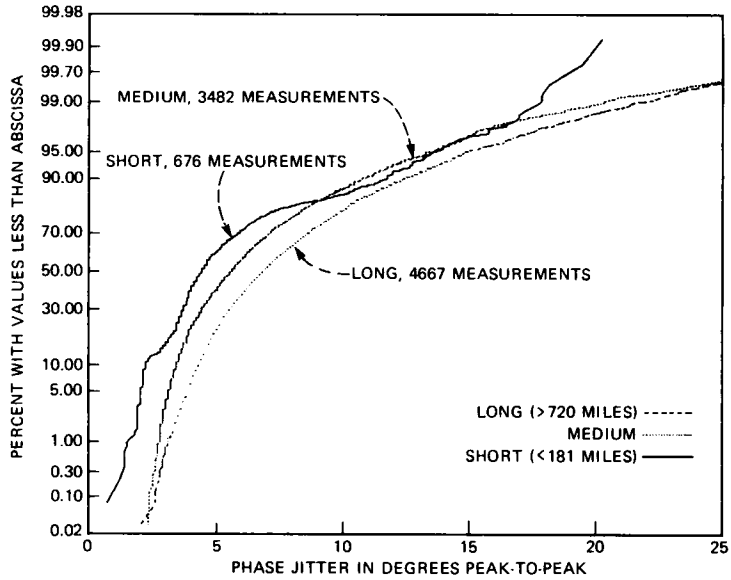

Fig. 39—CDFs of 2- to 300-Hz phase jitter for short, medium, and long mileage bands.

Figures 40 and 41 present the CDFs of amplitude jitter for the three mileage categories, for the two frequency bands, respectively.

Phase jitter can be caused by phase modulation as well as by noise. Measurement of phase jitter is appropriate to predict high-speed data set performance, but only as an indirect measure of phase modulation. However, the phase jitter measuring set alone cannot distinguish phase jitter caused by noise from that caused by phase modulation. The primary purpose of the amplitude jitter measurement is to separate phase jitter caused by the two sources.

Although both noise and amplitude modulation can cause amplitude jitter, a signal is unlikely to encounter amplitude modulation sources in the network, leaving noise as the sole source of amplitude jitter. On the other hand, the network has both sources for phase jitter, namely, noise and phase modulation. Therefore, the *amplitude* jitter measurements can be compared with *phase* jitter measurements to distinguish phase jitter caused by the two sources. For example, a high phase jitter measurement accompanied by a low amplitude jitter measurement on a connection is an indication that the phase jitter on that connection is not caused by noise, but most likely is caused by phase modulation.

Figure 42 is a scatter plot of the 20- to 300-Hz amplitude jitter versus the 20- to 300-Hz phase jitter. Also shown in the figure are two demarcation lines (labeled A and B) experimentally obtained by testing the phase and amplitude jitter measurement equipment used in the

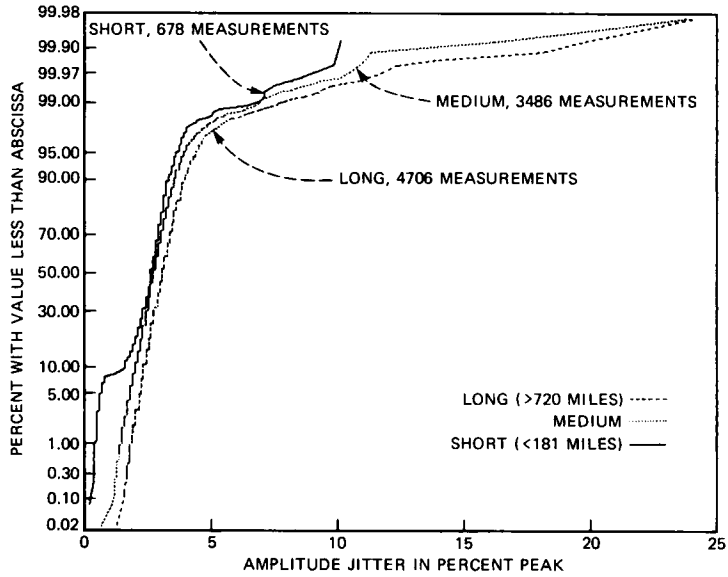

Fig. 40—CDFs of 20- to 300-Hz amplitude jitter for short, medium, and long mileage bands.

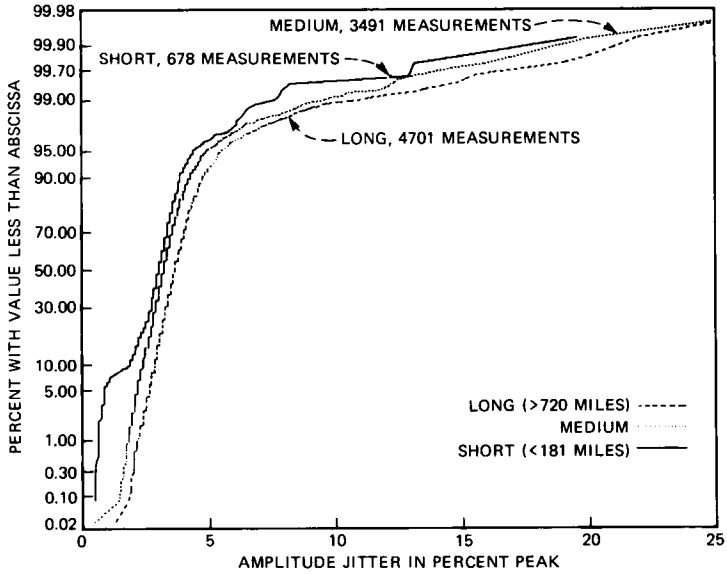

Fig. 41—CDFs of 2- to 300-Hz amplitude jitter for short, medium, and long mileage bands.

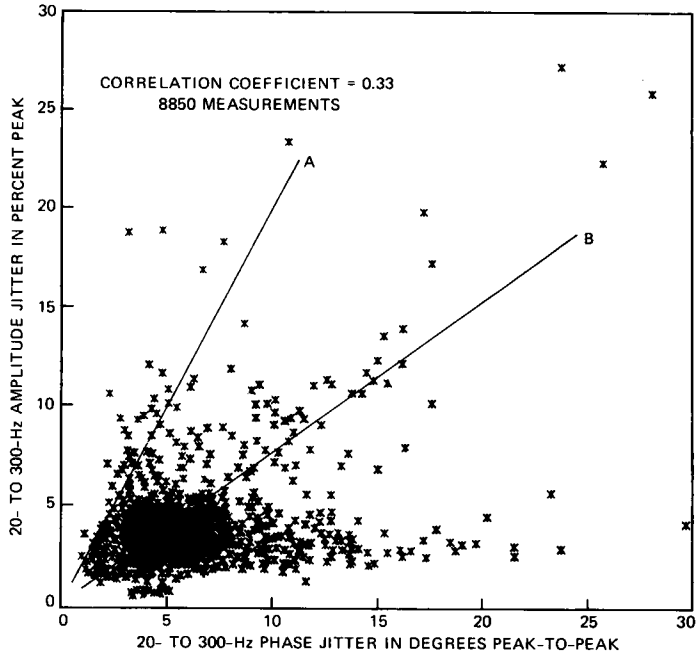

Fig. 42—Amplitude versus phase jitter in the 20- to 300-Hz band.

EOCS. Points between lines A and B indicate connections where phase and amplitude jitter show good correlation. Therefore, these points almost all correspond to phase jitter solely caused by noise. Points above line A show connections with high amplitude jitter but little phase jitter, and they are attributed to the effect of impulse noise on the amplitude jitter detector. (The requirements for all jitter detectors mandate peak detectors, which also respond to momentary increases from impulse noise.) Points below line B, showing connections with high phase jitter but low amplitude jitter, suggest that phase jitter on those connections is largely caused by phase modulation, and is occasionally caused by impulse noise.

3.9 Frequency shift

Frequency shift, or absolute frequency offset, is a critical parameter, for example, for the proper functioning of echo cancelers. Echo cancelers continue to adapt during voice calls and can track frequency shifts below 1 Hz. Depending on the magnitude of the frequency shift, brief transient echoes may be heard after conversational pauses, since adaptation only occurs when just one party is talking. Since echo cancelers freeze on calls where a continuous data set signal is present, frequency shift will cause echoes whose magnitudes change at the frequency shift rate.

Frequency shift was measured in the 1969/70 Connection Survey by transmitting at −12 dBm a 1200-Hz tone whose frequency was known to 0.1 Hz. The frequency of the received tone was measured to a precision of 0.1 Hz at the far end of the connection leading to an overall accuracy of approximately 0.2 Hz. The difference between the two frequencies was the frequency shift of the connection. The measured frequency shifts were not normally distributed. An offset of greater than 3 Hz was observed on two of the 600 measurements.

In the EOCS, the transmitted frequencies were known to a precision of 0.1 Hz. The received frequencies were measured to a resolution of 1 Hz with a frequency counter that could be momentarily driven upward by impulse noise, and could momentarily be driven downward by transient power line harmonics. Connections with poor s/n caused a positive 1-Hz offset in the frequency counter output. Taking only those connections for which multiple, stable frequency shifts were observed:

1. A positive frequency shift of 2 Hz was observed on eight of 4222 connections (0.19 percent).
2. A negative frequency shift of 1 Hz was observed on ten of 4222 connections (0.24 percent).

All but one of the stable frequency shifts observed were for connections to a single end office that had N3 (frequency division multiplex) carrier toll-connecting trunks. The precision of the frequency measurements in the EOCS is not sufficient to draw conclusions about the performance of the network for frequency shift, particularly since the observed shifts were associated with the toll-connecting trunks for a single office.

3.10 Impulse noise

Impulse noise was measured through a C-notched filter by counting the number of times the noise exceeded a given threshold. The impulse noise measurement consisted of three five-minute measurements in sequence, with three different thresholds for each five-minute interval.

The thresholds for impulse noise counts were set based on the received rms level of the 1004-Hz holding tone. For the first five minutes, thresholds were set at −12, −8, and −4 dB relative to the received holding tone level; for the second five minutes, at −12, −4, and +4 dB; for the last five minutes, at −8, 0, and +8 dB. Since measurements at the −12, −8, and −4 dB thresholds were made twice for five minutes on each connection, while measurements at the 0, +4, and +8 dB thresholds were made only once for five minutes per connection, all figures and results in this section are based on twice as many observations for the −12, −8, and −4 dB thresholds than for the other three higher thresholds.

Impulse noise counters with multiple thresholds have the characteristic that a single impulse exceeding the highest threshold must also register on all the lower thresholds. This means that, in any given five-minute interval, the counter for the lowest threshold will have the same as or higher count than the counter for a higher threshold. As one would expect, the CDF of impulse noise counts at the −12 dB threshold falls to the right of the CDF at the −8 dB threshold. Since the thresholds were changed for each of the three five-minute transient measuring intervals, it is possile (but unlikely) that on any given connection, there could be a smaller count for the 0-dB threshold than for the 4-dB threshold, for example.

Statistically, the effect of connection airline mileage was found not to be significant on impulse noise count. The type of switch at either end of the connection was found to be a significant factor. Figures 43 through 45 show the CDFs of impulse noise counts per five-minute interval at various thresholds for different switch types (digital, crossbar, and step-by-step switches) at the measuring end office. The type of switch in the end office from which the tone was sent was taken into consideration through a weighting process based on predivestiture Bell System traffic statistics. A connection with a digital switch at the measuring end is expected to have fewer impulse noise counts than a connection with an electromechanical switch (crossbar, or step-by-step) in which the operation and release of adjacent relays can sometimes cause impulse noise.

The limiting bend in the CDF for the −12 dB threshold at approximately 2000 counts per five-minute interval in Fig. 45 might have been caused by power-line-hum pickup in the small rural step-by-step offices, which caused continuous impulse counts at the maximum counting rate of 420 counts per minute.

Figures 46 and 47 show the effect of switch type at both ends of the connection. Three types of switch were evaluated in the EOCS, leading to six nonordered pairs of switches when both end switches were taken into consideration. Figure 46 shows the percentage of impulse noise counts per five-minute interval for the −12 dB threshold for each of six different pairs of switches. The bars are divided, reading from the bottom up, as 0 counts, 1 to 10 counts, 11 to 20 counts, 21 to 50 counts, and more than 50 counts. The digital switch performs better than the crossbar, which is superior to the step-by-step, and this holds for either end of the connection. Figure 47 is similar to Fig. 46 except for the −4 dB threshold.

Figure 48 shows the impulse noise counts per five-minute interval for the −12 dB threshold at the step-by-step measuring end office switch plotted as a function of the time of day. It indicates an increase in the impulse noise counts in step-by-step offices during the busy

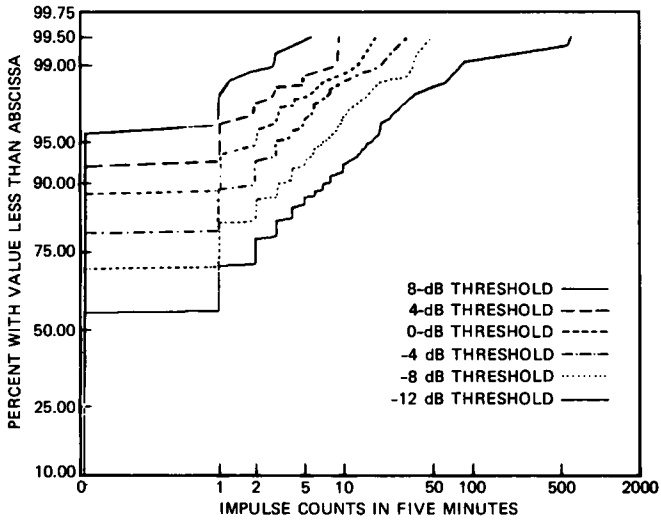

Fig. 43—CDFs of the impulse noise counts for the different thresholds as measured at electronic switching system end offices.

hours of a day, as one would expect when step-by-step switches in adjacent bays operate and release as other customers start and finish calls. A similar effect, with a smaller amplitude, was observed for the other thresholds and for the other types of switch.

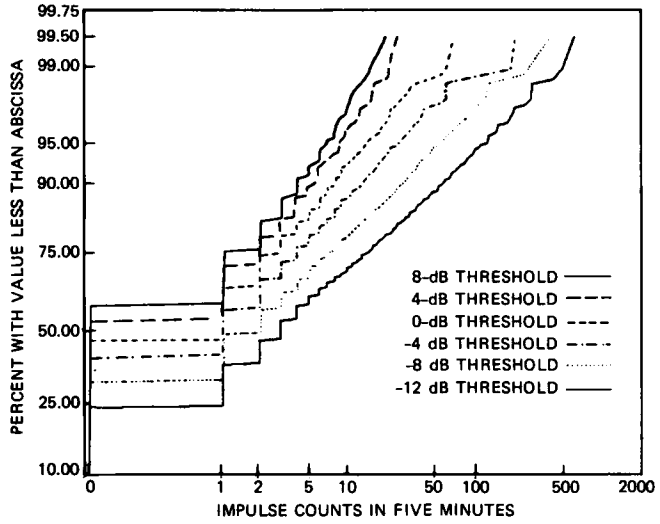

Fig. 44—CDFs of the impulse noise counts for the different thresholds as measured at crossbar end offices.

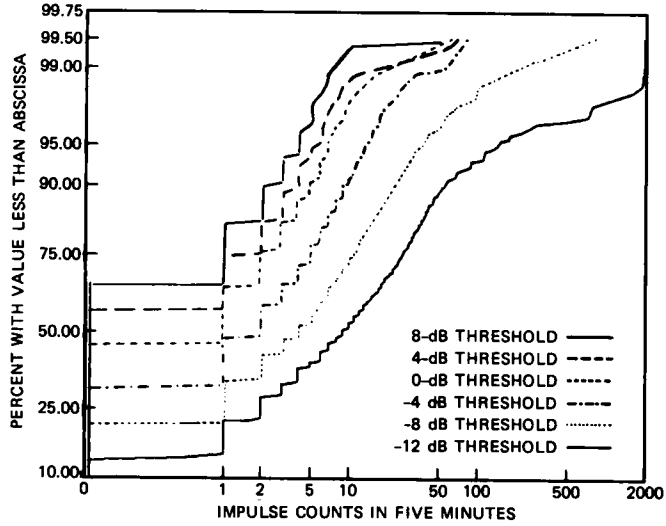

Fig. 45—CDFs of the impulse noise counts for the different thresholds as measured at step-by-step end offices.

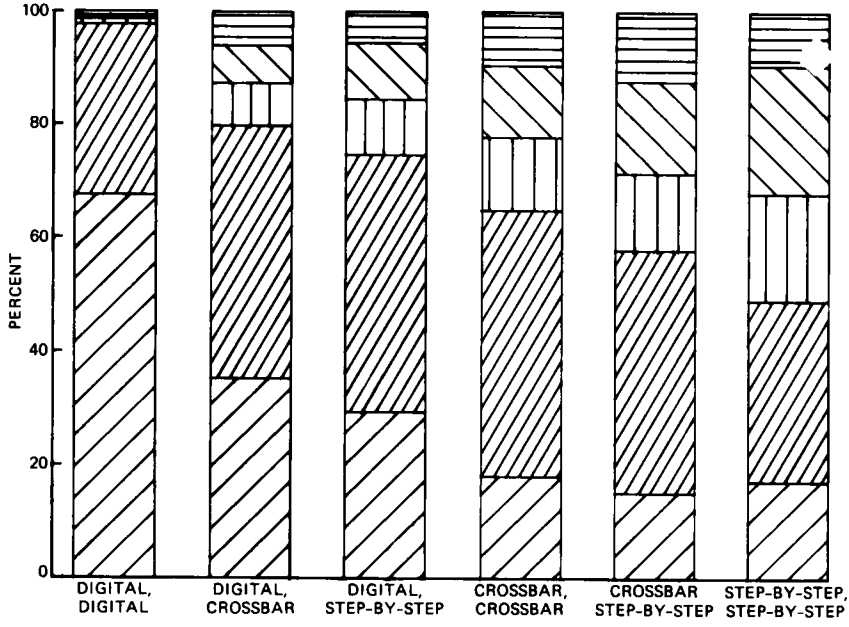

Fig. 46—Impulse noise counts for five-minute interval for the threshold of 12 dB below the received signal and for the six different pairs of end offices.

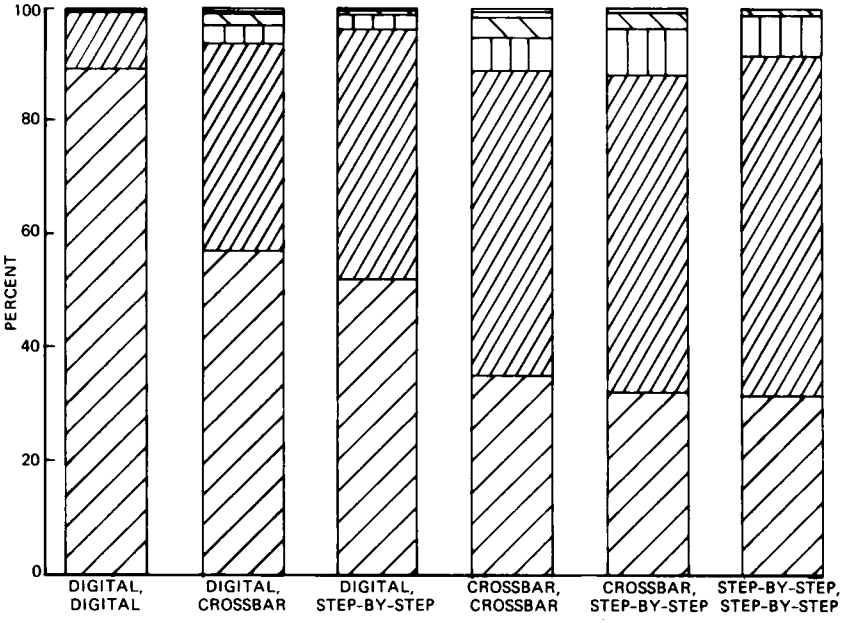

Fig. 47—Impulse noise counts per five-minute interval for the threshold of 4 dB below the received signal and for the six different pairs of end offices.

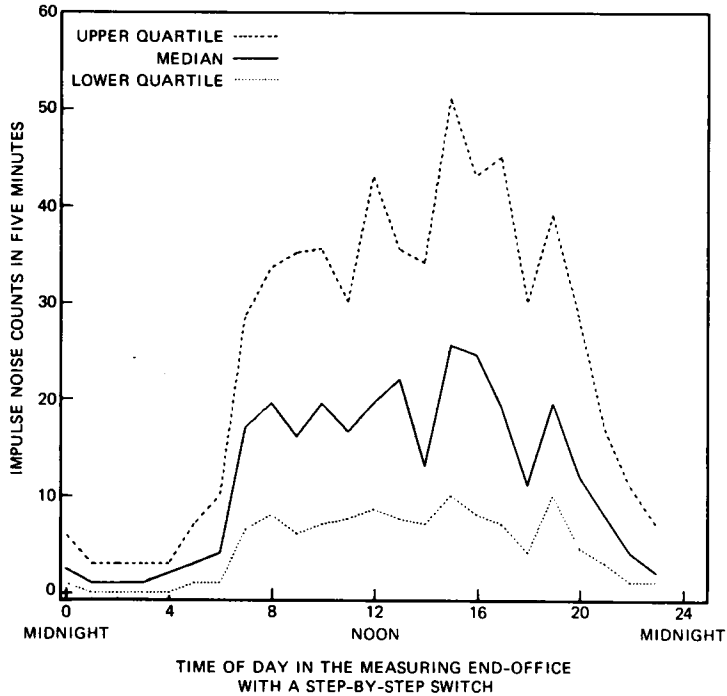

Fig. 48—Impulse noise counts for −12 dB threshold measured at step-by-step switches shown as a function of time of day.

3.11 Phase and gain hits

A phase hit is an abrupt change in the nominal phase of the received 1004-Hz holding tone lasting at least 4 ms. A gain hit is an abrupt change in the nominal level of the received 1004-Hz holding tone lasting at least 4 ms. The precision of the phase- and gain-hit measurement, the tracking rate for the phase-locked loop for the phase-hit counter, and the rate of change for the automatic gain control for the gain-hit counter are given in Ref. 1.

Phase and gain hits were measured simultaneously with impulse noise during the three five-minute transient measurement periods discussed in the previous section. During the first five minutes, the phase-hit threshold was set at 10 degrees and the gain hit threshold was set at 2 dB; during the second five minutes, the phase- and gain-hit thresholds were set at 15 degrees and 3 dB, respectively; finally, during the last five minutes, the phase- and gain-hit thresholds were set at 20 degrees and 6 dB, respectively. The phase- and gain-hit counting circuits respond to both positive and negative hits.

Figure 49 shows the CDFs of phase-hit counts per five-minute interval for the thresholds of 10, 15, and 20 degrees. The figure shows little difference between the CDFs corresponding to the two higher thresholds, 15 and 20 degrees. However, the CDF with 10-degree threshold is clearly worse than the other two CDFs. This may be caused by low-frequency phase modulation which can trigger the phase-hit counter at the 10-degree threshold.

Figure 50 shows the CDFs of gain-hit counts per five-minute interval for the thresholds of 2, 3, and 6 dB. There is a distinct reduction in the counts as the threshold is increased.

3.12 Dropouts

A dropout is defined as a 12-dB reduction of received signal level, as measured at the start of the 15-minute transient measurement interval, lasting for at least 4 ms. The dropout counter circuit has no automatic gain control circuit in contrast with the gain-hit counter. Figure 51 shows the CDF of dropout counts per 15-minute interval.

3.13 Bit and block error rates

The error rate performance of two widely used 1200-b/s data sets and two widely used 4800-b/s data sets was measured on the same connections on which the analog transmission impairments were measured. To simulate the environment in which the data sets would normally be operating, an artificial loop was placed in front of the data set in each ASPEN RTU. The artificial loop simulates 6000 feet of 26-gauge cable in series with 6000 feet of 24-gauge cable to achieve the mean loop loss of 5.3 dB determined from the 1980 Loop Survey. The data signal level at the data set was approximately −9 dBm.

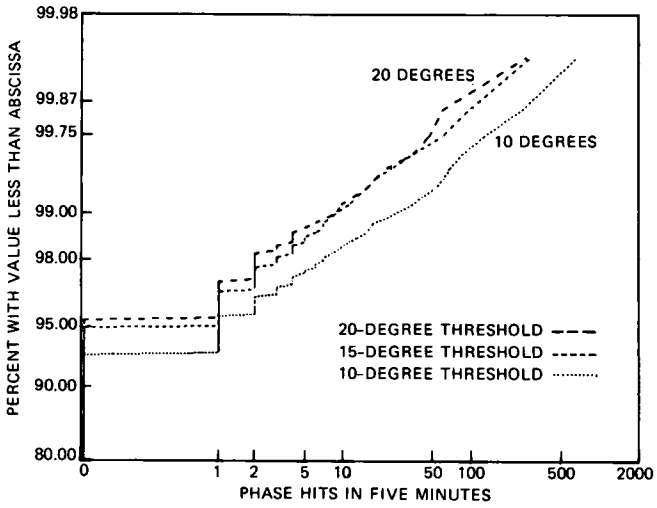

Fig. 49—CDFs of the phase hit counts for the thresholds of 10, 15, and 20 degrees.

The two 1200-b/s data sets used in the EOCS were full-duplex, four-phase, Differential Phase-Shift Keyed (DPSK) data sets. The data sets transmitted 1200-b/s (600-baud) synchronous binary serial data simultaneously in both directions by splitting the voiceband into a low band (carrier frequency of 1200 Hz) and high band (carrier frequency of 2400 Hz) of frequencies. The energy in the low-band line signal extended from 720 to 1680 Hz, and the high band, from 1920 to 2880 Hz. These data sets employed scramblers to prevent steady marking

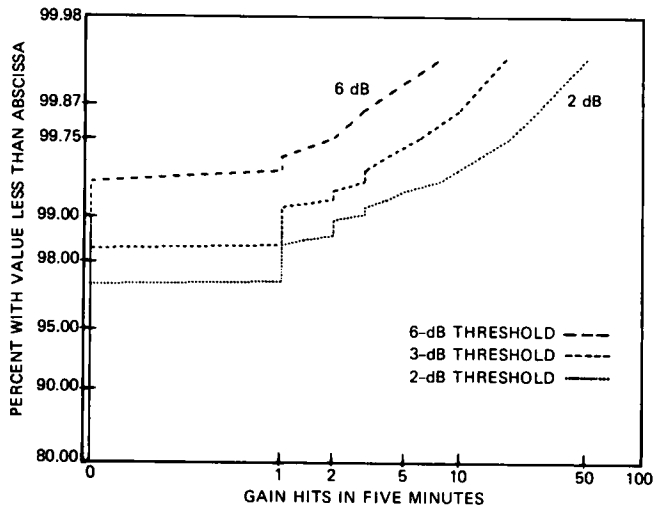

Fig. 50—CDFs of the gain-hit counts for the thresholds of 2, 3, and 6 dB.

or spacing to the transmitter causing a continuous stream of zero-degree phase shifts on the line (which would block the receiver timing-recovery circuit reference phase extraction from the incoming signal). These data sets had no adaptive equalizers to mitigate the effects of bandwidth reduction or poor EDD on the connection.

The two 4800-b/s data sets used in the EOCS were half-duplex, eight-phase DPSK data sets. They transmitted a 1600-baud (3 bits per symbol) signal, and 23-stage, multiple-tap scramblers were employed for the same reason as the scramblers in the 1200-b/s data sets. Most of the energy in the line spectrum was between 800 and 2800 Hz, and neither data set had a secondary channel. The receivers had adaptive equalizers to reduce the effects of connection bandwidth reduction and EDD on intersymbol interference.

The solid and dotted curves of Figs. 52, 53, and 54 show the CDFs of the bit error rates for the two 1200-b/s data sets for short, medium, and long connections. For these three figures, the low and high-band error rates were combined. The 1200-b/s data set bit error performance is poorer for longer connections. In Fig. 55, the bit error rates for long connections were separated into low and high band for the two 1200-b/s data sets. This figure demonstrates how the selection of the compromise equalizer in the data set can affect the relative performance of the two bands.

Since about one million bits were transmitted, there are no data points on the CDFs between "No Errors" and 1×10^{-6} bit error rate. The bit error rate counter in the ASPEN RTU attempted to resynchronize when 99 errors were received, and therefore the bit error rate plots were truncated at the value corresponding to 99 errors.

In the middle of the data collection period, the ASPEN RTUs were modified to permit both bit and block error rate measurement. For block error rate measurements, one thousand 1000-bit blocks were transmitted, and the restriction of no more than 99 errors in a single block was removed. All bit error rate figures include data collected over the entire EOCS data collection period, while the block error rate figures come from only the later part of the collection period. The CDFs for the block error rate performance for the two 1200-b/s data sets for short, medium, and long connections are shown in Figs. 56, 57, and 58. The block error rate performance of the 1200-b/s data sets is also poorer for the longer connections.

Figures 59, 60, and 61 show the bit error rate performance of the two 4800-b/s data sets for short, medium, and long connections.* As

* All error rate data presented here were taken with continuous carrier mode data set operation. Continuous carrier mode is the normal operation mode for the 1200-b/s full-duplex data sets. For the 4800-b/s half-duplex data sets, however, switched carrier mode is the typical mode of operation. In general, error performance with switched carrier mode operation is poorer than that with continuous carrier mode operation.

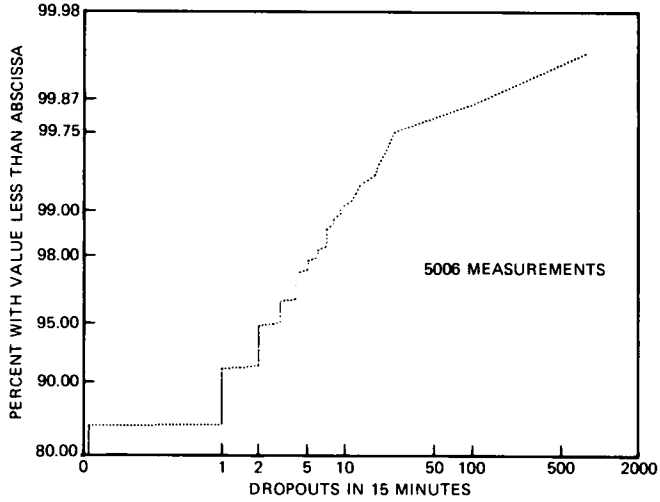

Fig. 51—CDF of dropout counts.

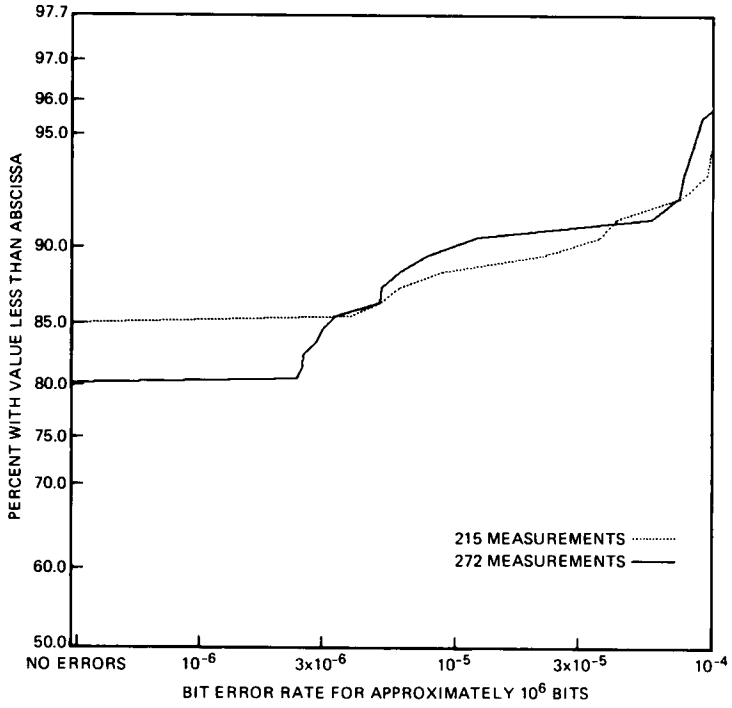

Fig. 52—CDFs of bit error rates for two 1200-b/s data sets for short connections.

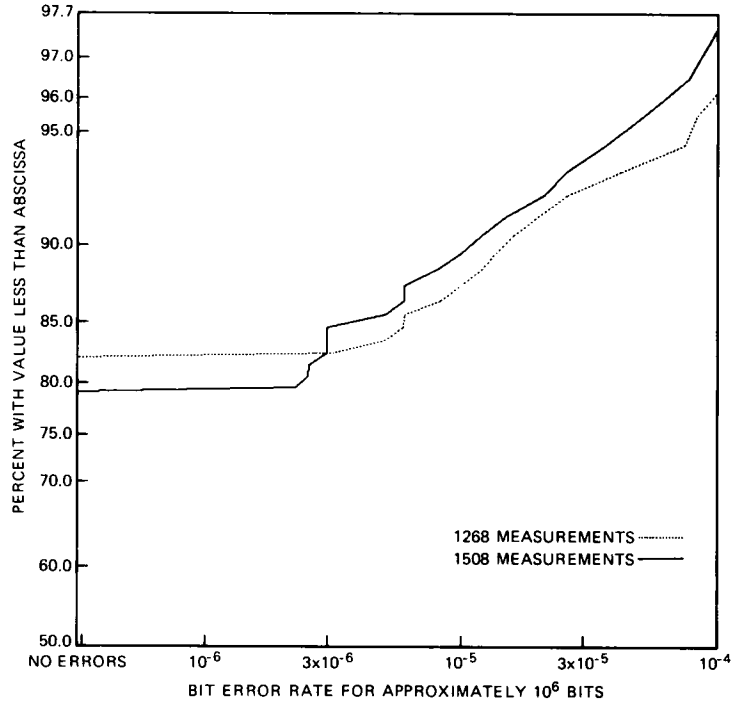

Fig. 53—CDFs of bit error rates for two 1200-b/s data sets for medium connections.

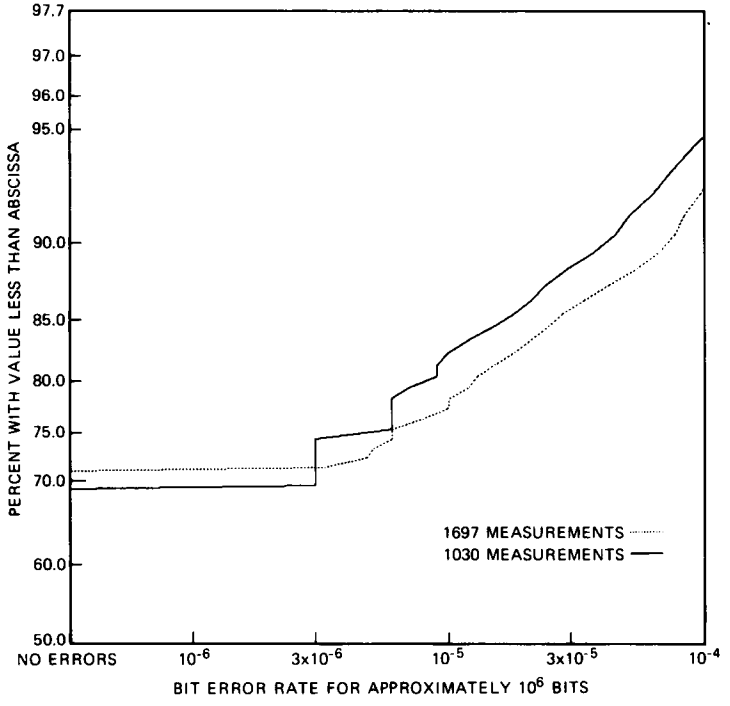

Fig. 54—CDFs of bit error rates for two 1200-b/s data sets for long connections.

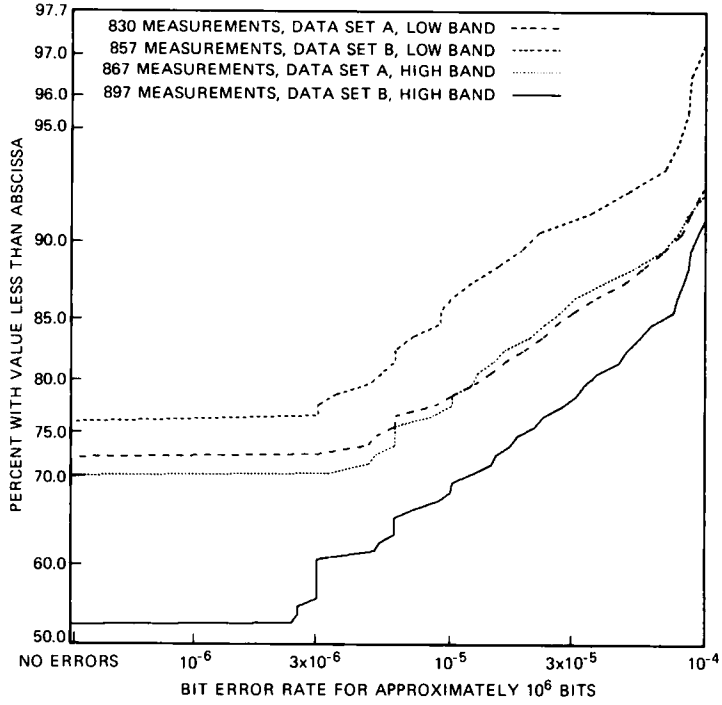

Fig. 55—CDFs for bit error rates for low and high bands for two 1200-b/s data sets for long connections.

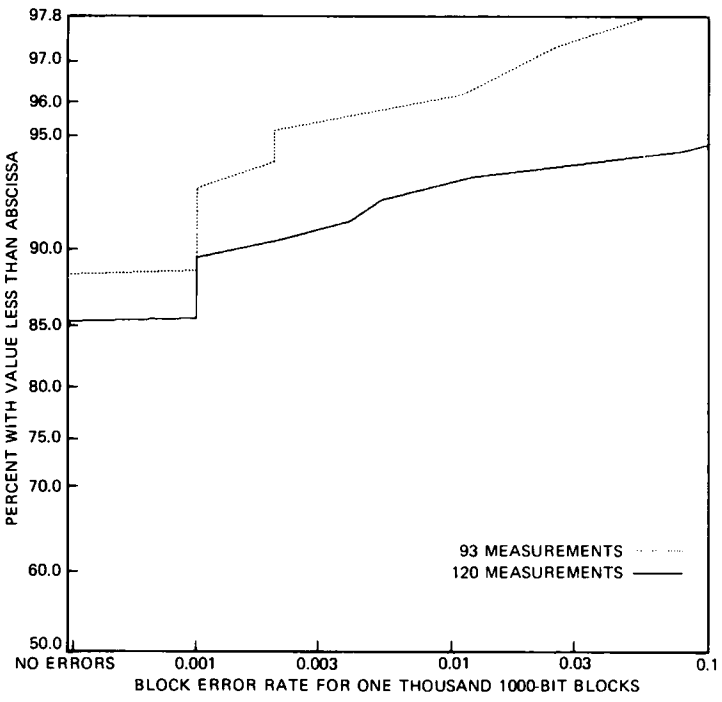

Fig. 56—CDFs of block error rates for two 1200-b/s data sets for short connections.

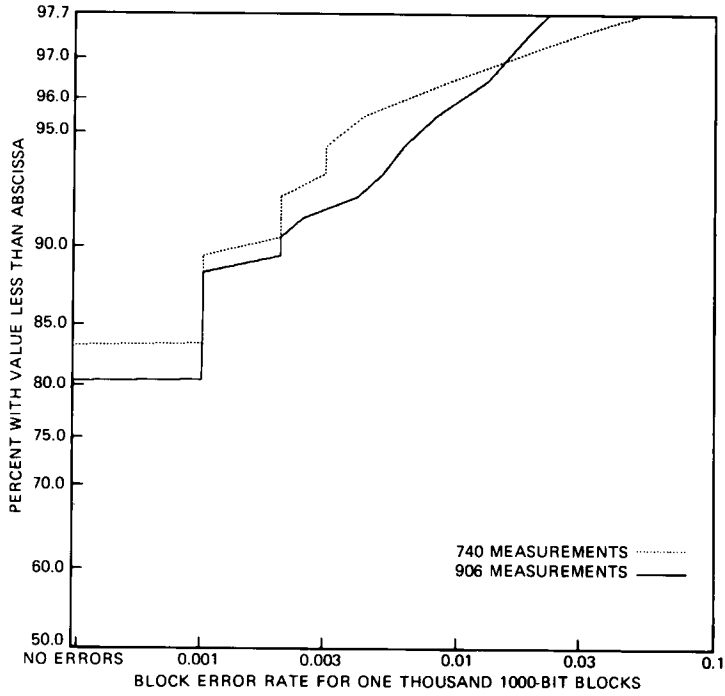

Fig. 57—CDFs of block error rates for two 1200-b/s data sets for medium connections.

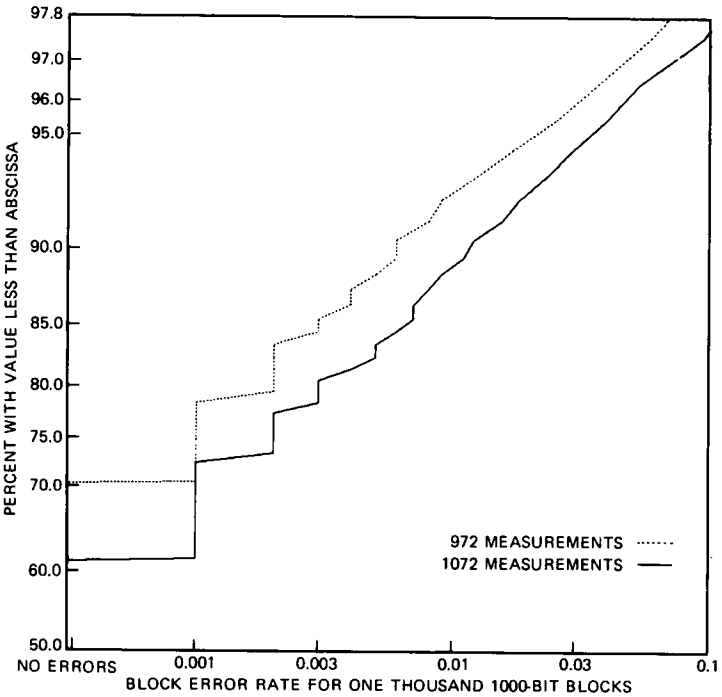

Fig. 58—CDFs of block error rates for two 1200-b/s data sets for long connections.

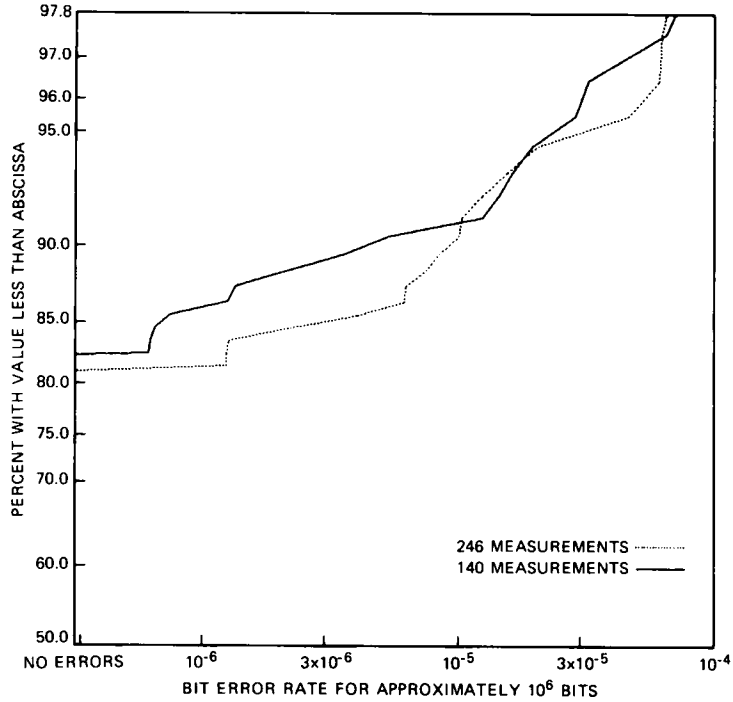

Fig. 59—CDFs of bit error rates for two 4800-b/s data sets for short connections.

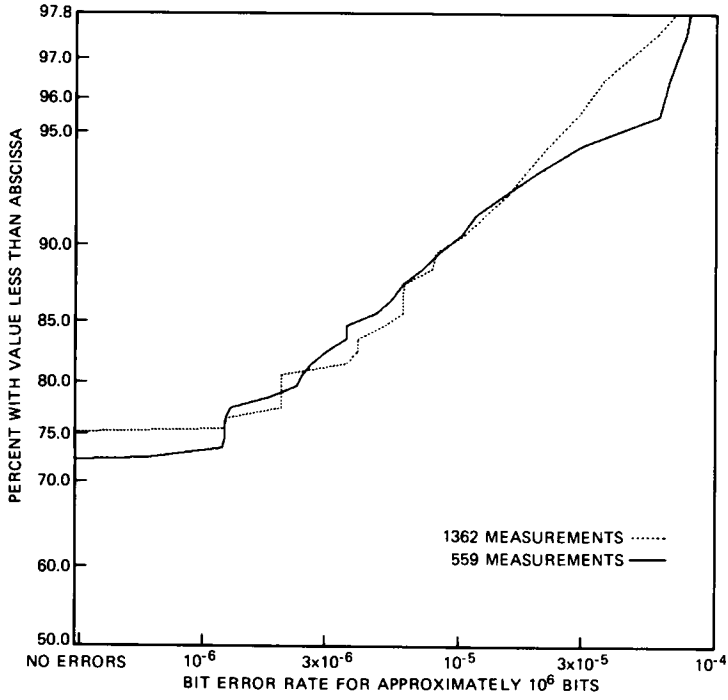

Fig. 60—CDFs of bit error rates for two 4800-b/s data sets for medium connections.

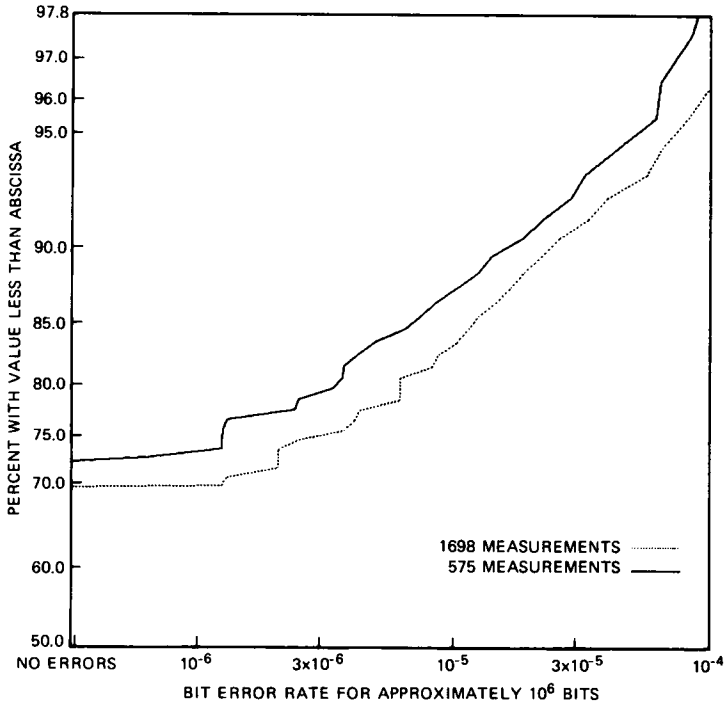

Fig. 61—CDFs of bit error rates for two 4800-b/s data sets for long connections.

we can see from the comparison of these figures and Figs. 52, 53, and 54, the bit error rates for the 1200-, and 4800-b/s data sets are not markedly different. This could be expected, considering that the much more expensive 4800-b/s data sets used in the EOCS had adaptive equalizers, and that the 1200-b/s, full-duplex data transmission is really two independent 1200-b/s data transmissions on the same connection.

The block error rate performance of one of the 4800-b/s data sets for short, medium, and long connections is shown in Fig. 62, once again demonstrating the poorer performance for long connections.

Figure 63 is a scatter plot of bit error rate versus block error rate for both of the 1200-b/s data sets, with a small amount of dither added in the horizontal axis to show where multiple points occur. As we can see from the line where errors occur in only one of the one thousand blocks (0.001), there is a preponderance of bit error counts of three, six, nine, and twelve. Figure 64 is a similar plot for one of the 4800-b/s data sets, which shows a tendency for an even number of error counts.

The figures that compare the two 1200-b/s data sets (or the two 4800-b/s data sets) show that there are differences in their perform-

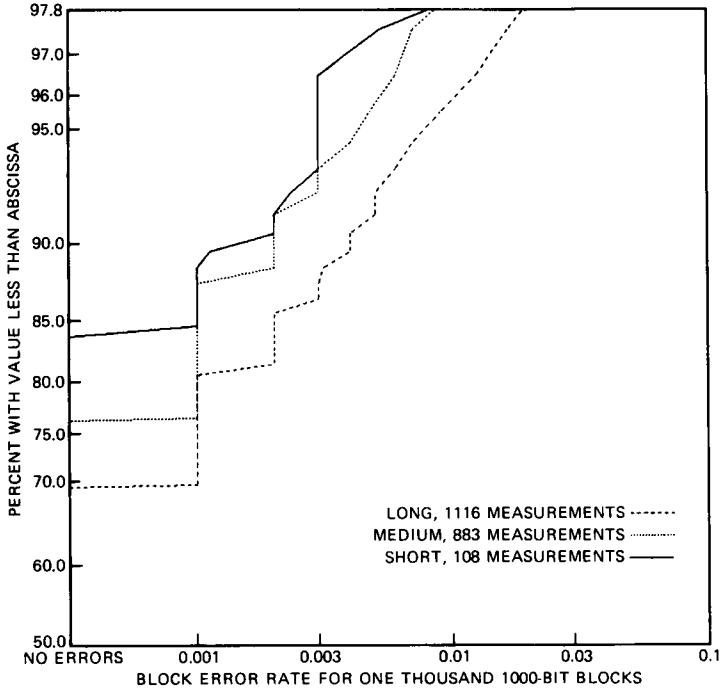

Fig. 62—CDFs for block error rate for a 4800-b/s data set for short, medium, and long connections.

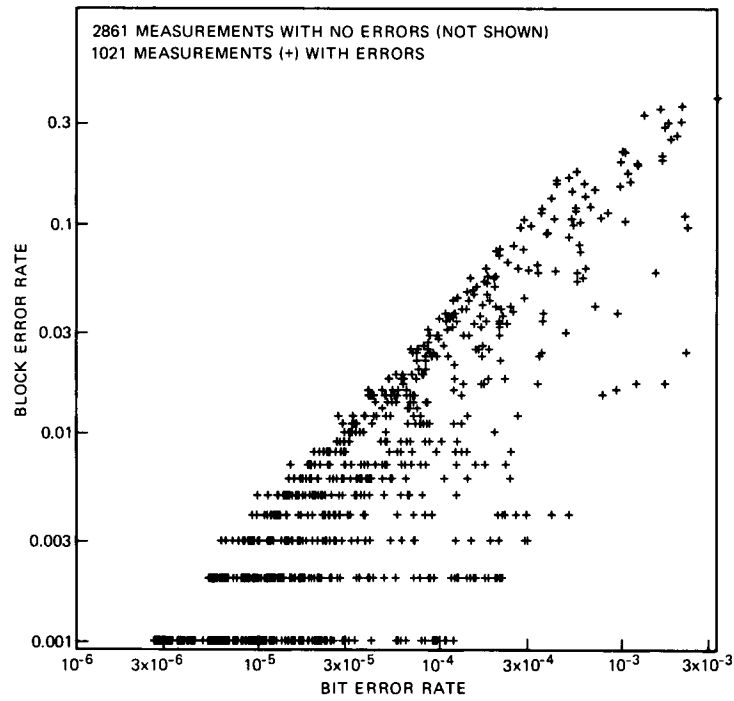

Fig. 63—Block error rate versus bit error rate for two 1200-b/s data sets for one thousand 1000-bit blocks.

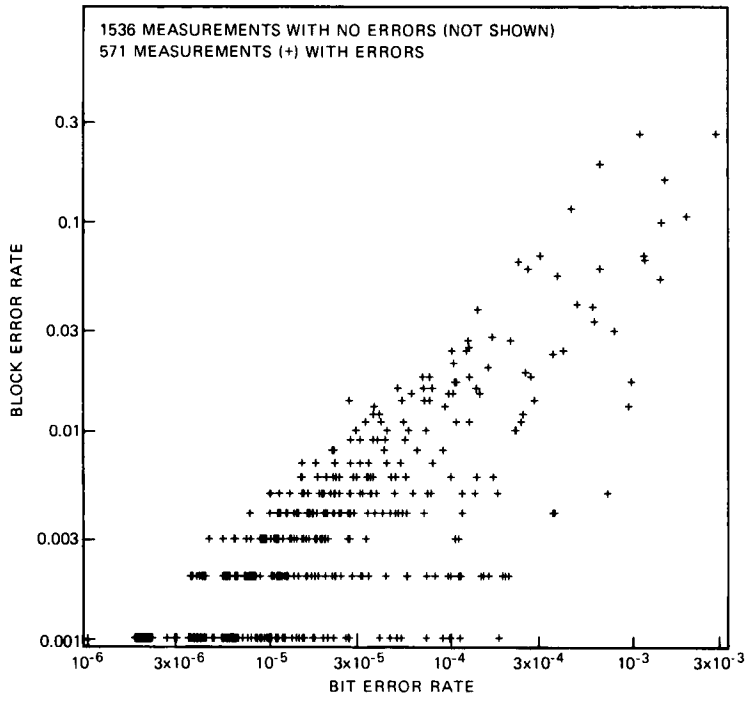

Fig. 64—Block error rate versus bit error rate for a 4800-b/s data set for one thousand 1000-bit blocks.

ance. Prediction of the performance of other types of data sets by extrapolation from these results is not warranted.

3.14 Cutoffs

The only nontransmission parameter estimated from the EOCS measurements is the call cutoff rate. A cutoff is a connection dropped prematurely; it can occur primarily because of failure in the communications path caused by transmission or switching problems. Failures resulting in carrier group alarms on T-carrier systems and talk off of in-band channel signaling are sources of transmission-caused cutoffs. Cutoffs caused by switching systems are the result of hardware failures, software failures (e.g., in digital switches), and procedural errors. The cutoff rate can be measured by examining a sample of representative connections through the network and observing the number of calls disconnected prematurely.

Four thousand toll connections were checked in the EOCS sample for possible cutoffs during the 15-minute intervals of impulse noise measurements discussed in Section 3.10. A cutoff was tallied if a call was disconnected at any time during the 15 minutes, given that the

call was up at the beginning of the same 15-minute interval. Twenty-two cutoffs occurred during the 60,000 call-minute sample (4000 × 15), leading to a nonweighted average cutoff rate of 2.2×10^{-3} for a six-minute holding time. The 90-percent confidence interval was calculated to be between 1.4×10^{-3} and 3.0×10^{-3}.

IV. ACKNOWLEDGMENTS

Many individuals contributed to the success of the ASPEN/End Office Connection Study (EOCS): Dave Leeper led the group that developed ASPEN and conducted the data acquisition phase of the EOCS; Jay MacMaster, Ed Vlacich, Al Furtado, and Jon Palmer designed, constructed, tested, and installed the ASPEN Remote Test Units (RTUs); Maurice Lampell, Louis Iacona, and Karel Ehrlich wrote and monitored the ASPEN central computer programs; Paul Auer designed the Transient Recording System and provided help in shaping the ASPEN system; Bob Sturges provided help in the design and construction of the RTU support circuitry; John Healy and Tom Redman developed the EOCS sampling plan; Blan Godfrey provided support for the original ASPEN concept; and Pete Lopiparo provided continued support throughout the completion of the ASPEN development, and the EOCS data acquisition and analysis. Finally, the cooperation and contributions of Bell Operating Company central office personnel are gratefully acknowledged.

REFERENCES

1. AT&T PUB 41009, *Transmission Parameters Affecting Voiceband Data Transmission—Measuring Techniques*, May 1975.
2. AT&T PUB 41008, *Transmission Parameters Affecting Voiceband Data Transmission—Description of Parameters*, July 1974.
3. J. D. Healy, M. Lampell, D. G. Leeper, T. C. Redman, and E. J. Vlacich, "1982/83 End Office Connection Study: ASPEN Data Acquisition System and Sampling Plan," AT&T Bell Lab. Tech. J., this issue.
4. F. P. Duffy and T. W. Thatcher, Jr., "1969–70 Connection Survey: Analog Transmission Performance on the Switched Telecommunications Network," B.S.T.J., *50*, No. 4 (April 1971), pp. 1311–47.
5. S. R. Searle, *Linear Models*, New York: Wiley, 1971, pp. 340–60.
6. R. Vernon, private communication.
7. T. C. Redman, private communication.
8. D. V. Batorsky and M. E. Burke, "1980 Bell System Noise Survey of the Loop Plant," AT&T Bell Lab. Tech. J., *63*, No. 5 (May-June 1984), pp. 775–818.
9. T. C. Anderson and D. L. Favin, *The P/AR Meter*, 1964 IEEE Int. Conv. Rec., *12*, Part 5, pp. 155–65.

AUTHORS

Michele B. Carey, B.S. (Mathematics), 1968; M.S. (Statistics), 1970, University of Sciences of Jussieu, Paris, France; Ph.D. (Applied Mathematical Sciences), 1982, University of Rhode Island; Bell Laboratories, 1982–1983. Present affiliation Bell Communications Research, Inc. Ms. Carey was involved in the data analysis of field measurements of the performance of the predivestiture Bell System telephone network. She is now involved in the

design and analysis of field studies aiming at the characterization of the transmission performance of the telephone network.

Han-Tee Chen, B.S. (Chemistry), 1970, Tsing Hua University, Taiwan; M.S. (Physical Chemistry), 1973, Worcester Polytechnic Institute, MA. Bell Laboratories, 1980–1983. Present affiliation Bell Communications Research, Inc. Ms. Chen designed and developed databases for network performance surveys and analyzed the results from those surveys. She is currently working on the software design and development of an automated reliability prediction system in the Methods and Information Division of Bell Communications Research.

Alfred Descloux, Diploma (Mathematics and physics), 1948, Swiss Federal Institute of Technology, Zurich, Switzerland; Ph.D. (Mathematics Statistics), 1961, University of North Carolina; Bell Laboratories, 1956–1983. Present affiliation Bell Communications Research, Inc. Mr. Descloux has been concerned with the probabilistic aspects of telephone traffic. In particular, his past work included new analytical results in the area of traffic measurements. Mr. Descloux is presently studying the performance of switching networks with integrated voice and data traffic. Member, American Mathematical Society, Institute of Mathematical Statistics.

James F. Ingle, B.S. (Electrical Engineering), 1955, Rensselaer Polytechnic Institute; M.S. (Electrical Engineering), 1961, New York University; Bell Laboratories, 1955–1983. Present affiliation Bell Communications Research, Inc. Mr. Ingle designed transmission test equipment for assessing the quality of video and voice transmission facilities. He holds seven patents in the test equipment field, and he wrote the Bell System technical reference for voiceband transmission test equipment (AT&T PUB 41009). Mr. Ingle is presently interpreting survey measurement results. He is a member of the IEEE subcommittee working on voiceband transmission test equipment requirements.

Kun I. Park, B.S. (Electrical Engineering), 1966, Seoul National University; M.S. (Electrical Engineering), 1968, Ph.D. (Electrical Engineering), 1972, University of Pennsylvania; Bell Laboratories, 1973–1983. Present affiliation Bell Communications Research, Inc. At Bell Laboratories, Mr. Park was Supervisor of the Data Communications Performance Characterization group, and he worked on data communications performance objectives and characterizations. He is now District Manager of the Data Services Performance District at Bell Communications Research, and he is responsible for performance planning for data services. His current projects include ISDN performance planning, field performance characterizations, construction of digital and voiceband data performance laboratories, and development of computer tools for circuit- and packet-switched data performance analysis. Member, IEEE, Sigma Xi.